VIBRATION CONFINEMENT PHENOMENA IN DISORDERED, MONO-COUPLED, MULTI-SPAN BEAMS

Djamel Bouzit
Graduate Student

Christophe Pierre
Assistant Professor

MEAM Report 91-02

Department of Mechanical Engineering and Applied Mechanics
The University of Michigan
Ann Arbor, Michigan 48109-2125 U.S.A.

Corresponding author:

Christophe Pierre
3200 G.G. Brown Building
Department of Mechanical Engineering and Applied Mechanics
The University of Michigan
Ann Arbor, MI 48109-2125
Tel: (313) 763-6853
Fax: (313) 747-3170

engn
UHR 0523

ABSTRACT

The effects of small, periodicity-destroying irregularities on the dynamics of multi-span beams are examined. It is shown that minute deviations of the span lengths from an ideal value alter qualitatively the dynamic response by *localizing* vibrations and waves to small geometric regions. These confinement phenomena are studied over a wide frequency range for beams resting on simple supports and with variable interspan coupling. Approximations of the localization factor (the average rate of spatial exponential decay of the vibration amplitude) are derived by statistical perturbation methods and validated by Monte Carlo simulations. If the interspan coupling is strong, localization effects are weak and of no practical significance for most engineering structures. On the other hand, localization is severe for small interspan coupling. Confinement is also generally stronger near the edges of frequency passbands and increases nearly linearly with frequency from passband to passband. This means that strong localization occurs at high frequencies, even for large static coupling between spans. De-localization is also observed at very high frequencies.

NOMENCLATURE

C	torsional spring stiffness constant
E	Young's modulus
i^2	$\equiv -1$
I	area moment of inertia
j	span number
ξ	wave number
K	$\equiv Cl_o/2EI$
l_j	length of span j
l_o	nominal, or average span length
$\bar{l}_j$	$\equiv l_j/l_o$
m	mass per unit length
M_j	moment at left end of span j
$\overline{M}_j$	$\equiv M_j l_o/EI$, dimensionless bending moment
N	number of spans
p	$\equiv \sqrt{\bar{\omega}}$
$\mathbf{T}_j$	$\equiv \mathbf{T}(\bar{l}_j)$ random transfer matrix for span j
$\mathbf{T}_o$	$\equiv \mathbf{T}(1)$ average, or nominal, transfer matrix
$\mathbf{W}_j$	$\equiv \mathbf{W}(\bar{l}_j)$ random wave transfer matrix for span j
$\mathbf{W}_o$	$\equiv \mathbf{W}(1)$ average, or nominal, wave transfer matrix
$2w$	width of the uniform probability density function of disorder
$\mathbf{X}$	matrix of eigenvectors of $\mathbf{T}_o$
x	distance along a span
y	transverse deflection
γ	localization factor
λ	eigenvalue of transfer matrix
$\bar{\omega}$	$\equiv \omega/\sqrt{EI/ml_o^4}$, dimensionless frequency
σ	standard deviation of disorder
θ_j	slope at left end of span j
$< . >$	average of a random variable

1. INTRODUCTION

Periodic structures consist of identical subsystems repeated along one or more directions and coupled through one or more coordinates. Many engineering structures are periodic—for example: truss beams; turbomachinery rotors; airframes; towed-array sonars; and laminated composites. The general purpose of this research is to examine how the dynamics of such structures is affected by small irregularities that destroy perfect periodicity. In this paper, we study a simple multi-span structure with imperfections, *i.e.* a multi-span beam on rigid supports that are randomly spaced.

Periodic structures have characteristic properties that make much of their dynamics qualitatively the same. These were studied first by Brillouin (1953) in a pioneering work, and later by Heckl (1964) and Mead (1971, 1975). Periodic structures feature alternating frequency bands in which harmonic waves either propagate freely (passbands) or are attenuated (stopbands). The number of passbands equals the number of degrees of freedom (DOF) of a subsystem and energy is transmitted along the structure only in the passbands. There are as many pairs of waves as there are coupling coordinates between two adjacent subsystems, and each pair of waves is characterized by a *propagation constant*, μ, such that waves propagate according to $e^{\pm\mu}$. For example, a Euler-Bernoulli beam on rigid supports is mono-coupled through the rotation at the supports and thus features a single propagation constant, while a beam on flexible supports is bi-coupled, as energy also transmits through the bending displacement at the supports. The natural frequencies of an N-bay periodic structure typically lie within the passbands, with N frequencies in each passband. For example, for beams on rigid supports, Miles (1956) was first to show that the natural frequencies of an N-span beam are clustered in an infinite number of bands, with N frequencies in each band. The mode shapes of periodic structures are extended and feature a nonattenuated shape.

The design and analysis of periodic engineering structures is usually based on the assumption that periodicity is perfect. However, departure from periodicity always occurs because of manufacturing and material tolerances. These irregularities may severely alter the structure's dynamics by confining the vibrational energy to small geometric regions, a phenomenon known as *normal mode localization.*

Mode localization was first predicted in solid state physics by Anderson (1958) and has been examined in structural dynamics only recently. The work of Hodges (1982) was ground-breaking and laid the foundations for most of what followed; for example, the works of Hodges and Woodhouse (1983), Pierre and Dowell (1987), Pierre (1988, 1990), Bendiksen (1987), and Cornwell and Bendiksen (1989). The dissertation of Kissel (1988) provides a nice account of this history and the most recent contributions. Research on localization has focused chiefly on the deterministic study of localized free modes and on the statistical analysis of the confinement of harmonic waves and vibrations near the excitation source. In most studies some type of perturbation or Taylor expansions were used to approximate either the localized free modes or the rate of spatial decay of the vibration amplitude.

While a number of studies of *periodic* multi-span beams were performed in the past (see (Mead, 1970), (Mead and Markuš, 1983), (Miles, 1956), (Lin and McDaniel, 1969), (Tassilly, 1987), (Faulkner and Hong, 1985), and (Sen Gupta, 1970)), localization in multi-span structures was first examined by Pierre *et al.* (1987) for a simple two-span beam, both theoretically and experimentally. The study showed that localization occurs for weak coupling between spans when the intermediate support is located slightly away from the middle of the beam. Kissel (1988) made an important contribution by deriving approximate

localization factors (the average rate of spatial decay of the amplitude) for multi-span beams on randomly spaced rigid supports. His model, however, did not allow for variable coupling between spans and, consequently, his results were mostly concerned with weak localization effects. In a very recent study, Cai and Lin (1990) calculated localization factors for a multi-span beam on equally spaced rigid supports by a new perturbation technique, but they examined the effects of randomness in the torsional stiffness of the intermediate supports. Also recently, Lust *et al.* (1990) studied localization numerically in multi-span beams on flexible supports using a Timoshenko beam model. Finally, it should be pointed out that multi-span beams on randomly spaced supports were studied earlier by Lin and Yang (1974). However, although they demonstrated the high sensitivity of the dynamics to the break in periodicity, they did not evidence localization.

In this paper, we examine localization phenomena in mono-coupled, multi-span beams with small random variations of the span lengths. A key feature of our approach is that we allow for *variable coupling* between the spans, which allows us to examine both weak and strong localization effects. This is achieved in our model by including torsional springs at the supports. We show that for the transmission of vibrations to be severely affected by the small randomness in support spacing, either *the interspan coupling must be weak* or *the frequency must be high.* The paper is organized as follows. We begin with the problem formulation in Section 2. In Section 3 we review results for the perfectly periodic multi-span beam. In Section 4 we calculate localization factors by statistical perturbation methods for cases of weak and strong interspan coupling. We compare these results with Monte Carlo simulations in Section 5. In Section 6 we examine localization effects at high frequencies and Section 7 contains concluding remarks.

The main contribution of this paper is the study of localization in a multi-span beam with randomly spaced supports *and* with variable coupling. In particular, the results we obtain for weak interspan coupling are new. Also new are our results regarding the variation of localization effects as frequency increases, both for moderate and high frequencies.

2. PROPAGATION CONSTANTS AND LOCALIZATION FACTORS

We consider the undamped, (nearly) periodic beam on simple supports shown in Fig. 1. We assume the beam is uniform and homogeneous throughout its entire length, consider only bending motion and neglect shear deformation. The (identical) linear torsional springs that exert restoring moments at the supports allow us to vary the coupling between spans. For example, as the torsional stiffness approaches infinity, the transmission of bending moment reduces to zero and the interspan coupling vanishes. We define the beam as ordered if all spans have identical lengths and create disorder by varying the locations of the supports in a random fashion. We restrict our analysis to *small* span length deviations about a nominal value.

In this section, we characterize the transmission of a free harmonic wave of frequency ω through the multi-span beam. We also consider an alternative formulation where the beam is excited at one end with a harmonic force and the steady state response at the other end is examined. In both cases we obtain the transmission properties of *infinite* multi-span beams, which is a limitation of the approach.

2.1 Transfer Matrix for the Mono-Coupled, Multi-Span Beam

We first derive a transfer matrix that relates the dynamics at two adjacent spans. Since the beam rests on simple supports, the individual spans possess a single DOF at each end.

This means that the beam is *mono-coupled* and its dynamics can be represented by 2×2 transfer matrices. Here we choose to describe the vibrational state at a support by the slope and the bending moment. A span of length l_j is shown in Fig. 2, where θ_{L_j} (*resp.* θ_{R_j}) and M_{L_j} (*resp.* M_{R_j}) are the slope and the bending moment at the left end (*resp.* right end). Considering free motion in the jth span, the bending deflection is, from Euler-Bernoulli theory

$$y_j(x) = A_1 \cosh(\beta x) + A_2 \sinh(\beta x) + A_3 \cos(\beta x) + A_4 \sin(\beta x) \qquad x \in [0, l_j] \tag{1}$$

where $\beta = \sqrt{\omega}\,(\frac{m}{EI})^{\frac{1}{4}}$. The coefficients in Eq. (1) are obtained by applying the conditions at the span ends

$$y_j(0) = 0\,,\ \theta_j(0) = \theta_{L_j}\,,\ y_j(l_j) = 0\,,\ \theta_j(l_j) = \theta_{R_j} \tag{2}$$

where the bending slope is $\theta_j(x) = \frac{dy_j}{dx}(x)$. The left- and right-end bending moments are given by

$$\begin{cases} M_{L_j} = -EI\frac{d\theta_j}{dx}(0) + \frac{C}{2}\theta_{L_j} \\ M_{R_j} = EI\frac{d\theta_j}{dx}(l_j) + \frac{C}{2}\theta_{R_j} \end{cases} \tag{3}$$

Substituting $\theta_j(x)$ obtained above in terms of θ_{L_j} and θ_{R_j} gives two relations between the moments and slopes at the ends of span j

$$\begin{bmatrix} \overline{M}_{L_j} \\ \overline{M}_{R_j} \end{bmatrix} = \begin{bmatrix} \frac{p}{\alpha_j} g_j + K & -\frac{p}{\alpha_j} \\ -\frac{p}{\alpha_j} & \frac{p}{\alpha_j} g_j + K \end{bmatrix} \begin{bmatrix} \theta_{L_j} \\ \theta_{R_j} \end{bmatrix} \tag{4}$$

where $\overline{M}_{L_j}$ and $\overline{M}_{R_j}$ are dimensionless bending moments, K the dimensionless torsional spring stiffness that governs the interspan coupling, and $p = \sqrt{\omega}$, all defined in the nomenclature. We define the function g_j by

$$g_j \equiv g(\bar{l}_j) = \frac{\sinh p_j \cos p_j - \cosh p_j \sin p_j}{\sinh p_j - \sin p_j} \tag{5}$$

where $p_j = p\bar{l}_j$, with $\bar{l}_j$ as the dimensionless span length. Finally, α_j is defined in Appendix A.

Next, we write that $\theta_{L_{j+1}} = \theta_{R_j}$ and $\overline{M}_{L_{j+1}} = -\overline{M}_{R_j}$. Defining the state vector for the jth span by the slope and the bending moment at its left end, $\theta_j \equiv \theta_{L_j}$ and $\overline{M}_j \equiv \overline{M}_{L_j}$, we obtain from Eq. (4) a transfer matrix that relates the dynamics at two adjacent supports

$$\begin{bmatrix} \theta_{j+1} \\ \overline{M}_{j+1} \end{bmatrix} = \mathbf{T}_j \begin{bmatrix} \theta_j \\ \overline{M}_j \end{bmatrix} \tag{6}$$

where

$$\mathbf{T}_j \equiv \mathbf{T}(\bar{l}_j) = \begin{bmatrix} g_j + \frac{\alpha_j}{p} K & \frac{-\alpha_j}{p} \\ \frac{p}{\alpha_j}(1 - g_j^2) - 2Kg_j - \frac{\alpha_j}{p} K^2 & g_j + \frac{\alpha_j}{p} K \end{bmatrix} \tag{7}$$

Clearly, $\det \mathbf{T}_j = 1$ for this undamped span. For a disordered beam the $\mathbf{T}_j$'s are random transfer matrices. For a tuned multi-span beam the individual spans' transfer matrices are identical and equal to

$$\mathbf{T}_o \equiv \mathbf{T}(< \bar{l}_j >) = \begin{bmatrix} g + \frac{\alpha}{p} K & -\frac{\alpha}{p} \\ \frac{p}{\alpha}(1 - g^2) - 2Kg - \frac{\alpha}{p} K^2 & g + \frac{\alpha}{p} K \end{bmatrix} \tag{8}$$

where $< \bar{l}_j >= 1$ is the nominal, or average dimensionless span length, $g \equiv g(1)$ and $\alpha \equiv \alpha(1)$.

2.2 Wave Formulation

Here we define the propagation constant and the localization factor based upon a traveling wave approach (see Kissel (1988) for a detailed derivation). We examine the propagation of a harmonic wave of frequency ω, through the beam and introduce wave amplitudes from the slope/moment state vector by the transformation

$$\begin{bmatrix} \theta_j \\ M_j \end{bmatrix} = \mathbf{X} \begin{bmatrix} L_j \\ R_j \end{bmatrix} \tag{9}$$

where L_j is the complex amplitude of the wave leaving span j to the left and R_j is that of the wave entering span j from the left (see Fig. 2). The columns of $\mathbf{X}$ are the eigenvectors of the transfer matrix for an ordered span, $\mathbf{T}_o$

$$\mathbf{X} = \begin{bmatrix} 1 & 1 \\ -i\frac{p}{\alpha}\sqrt{1-(g+\alpha K/p)^2} & +i\frac{p}{\alpha}\sqrt{1-(g+\alpha K/p)^2} \end{bmatrix} \tag{10}$$

Substituting Eq. (9) into Eq. (6) we obtain a wave transfer matrix that relates the wave amplitudes at adjacent supports

$$\begin{bmatrix} L_{j+1} \\ R_{j+1} \end{bmatrix} = \mathbf{W}_j \begin{bmatrix} L_j \\ R_j \end{bmatrix} \quad \text{with} \quad \mathbf{W}_j = \mathbf{X}^{-1}\mathbf{T}_j\mathbf{X} \tag{11}$$

In general the wave transfer matrix $\mathbf{W}_j$ is not diagonal, unless it corresponds to an ordered span. This means that disorder in the span lengths produces scattering that results in localization.

To eliminate reflections at the boundaries from our calculation, we consider a beam with an infinite number of spans in which an N-span disordered segment is embedded. Thus, we have $\bar{l}_j = 1$ for $-\infty < j \leq 0$ and $N < j < +\infty$ and random lengths $\bar{l}_j$ for $j = 1, \cdots, N$. This way we insure there is no reflection beyond the N-span segment.

The wave amplitudes entering and leaving the disordered segment are related by

$$\begin{bmatrix} L_{N+1} \\ R_{N+1} \end{bmatrix} = \mathcal{W}_N \begin{bmatrix} L_1 \\ R_1 \end{bmatrix} \tag{12}$$

where, for frequencies in the passbands,

$$\mathcal{W}_N = \prod_{j=N}^{1} \mathbf{W}_j = \begin{bmatrix} 1/t_N & -r_N/t_N \\ -r_N^*/t_N^* & 1/t_N^* \end{bmatrix} \tag{13}$$

where t_N and r_N are the transmission and reflection coefficients for the disordered segment and * denotes a complex conjugate.

If we consider a wave of amplitude α incident from the left, we have $L_{N+1} = 0$ and $R_1 = \alpha$, and a simple manipulation shows that the ratio of the amplitude transmitted through the disordered segment to the incident amplitude, R_{N+1}/α, equals the transmission coefficient t_N. If we assume that, asymptotically, the transmitted wave amplitude decays *exponentially* along the chain, we obtain the limit of the rate of decay per site as

$$\gamma = \lim_{N\to\infty} -\frac{1}{N} \ln |t_N| \tag{14}$$

which we define as the *localization factor* for the disordered structure. Asymptotically, Eq. (14) means that the magnitude of the transmission coefficient decays exponentially with N at the rate γ. For an ordered structure γ is the real part of the propagation constant. Note that if we assume ergodicity, γ can also be viewed as the average rate of decay for finite disordered multi-span beams

$$\gamma = \left\langle \frac{1}{N} \ln \left| \frac{1}{\tau_N} \right| \right\rangle \tag{15}$$

2.3 Vibration Formulation

Here the N-span beam is excited at its left end with a simple harmonic moment of frequency ω and dimensionless amplitude $\overline{M}$. Our interest lies in the transmission of steady-state vibrations along the beam.

Using Eq. (4) that relates the moments and slopes at both ends of a span for the $(j-1)$th and the jth span, we can eliminate the bending moments by using the continuity condition $\overline{M}_{R_{j-1}} = -\overline{M}_{L_j}$. This yields a recursive expression relating the slope amplitudes at three adjacent supports:

$$-\frac{p}{\alpha_{j-1}}\theta_{j-1} + \left(2K + \frac{pg_j}{\alpha_j} + \frac{pg_{j-1}}{\alpha_{j-1}}\right)\theta_j - \frac{p}{\alpha_j}\theta_{j+1} = 0 \tag{16}$$

This can be written in matrix form, for the N-span beam, as

$$\mathbf{A}\begin{bmatrix} \theta_1 \\ \theta_2 \\ \vdots \\ \theta_{N+1} \end{bmatrix} = \begin{bmatrix} \overline{M} \\ 0 \\ \vdots \\ 0 \end{bmatrix} \tag{17}$$

where $\mathbf{A}$ is the tridiagonal matrix

$$\mathbf{A} = \begin{bmatrix} K + \frac{pg_1}{\alpha_1} & -\frac{p}{\alpha_1} & & & & & \\ \ddots & \ddots & \ddots & & & 0 & \\ & \ddots & \ddots & \ddots & & & \\ & & -\frac{p}{\alpha_{j-1}} & 2K + \frac{pg_j}{\alpha_j} + \frac{pg_{j-1}}{\alpha_{j-1}} & -\frac{p}{\alpha_j} & & \\ & & & \ddots & \ddots & \ddots & \\ & 0 & & & \ddots & \ddots & \ddots \\ & & & & & -\frac{p}{\alpha_N} & K + \frac{pg_N}{\alpha_N} \end{bmatrix} \tag{18}$$

The steady state response is simply obtained by inverting $\mathbf{A}$. The slope at the right end is of special interest in our study of localization and is given by

$$\frac{\theta_{N+1}}{\overline{M}} = \frac{[\text{ cofactor matrix of } \mathbf{A} \,]_{(1,N+1)}}{\det \mathbf{A}} = \frac{1}{\det \mathbf{A} \prod_{j=1}^{N} \alpha_j} \tag{19}$$

Assuming that asymptotically the slope amplitudes decay exponentially, we obtain the localization factor as

$$\gamma = \lim_{N\to\infty} -\frac{1}{N} \ln \left| \frac{\theta_{N+1}}{\overline{M}} \right| = \lim_{N\to\infty} \frac{1}{N} \left(\sum_{j=1}^{N} \ln |\alpha_j| + \ln |\det \mathbf{A}| \right) \tag{20}$$

To evaluate γ we need to calculate $\det \mathbf{A}$ as a function of frequency and then take the limit of its logarithm. In some cases closed-form approximations of γ can be obtained, where the determinant is calculated via modal analysis. In general the localization factor can be approximated numerically for long beams.

3. WAVE PROPAGATION IN THE ORDERED MULTI-SPAN BEAM

The propagation of waves in the infinite ordered multi-span beam is governed by the eigenvalues of the transfer matrix $\mathbf{T}_o$:

$$\lambda_1 = (g + \alpha K/p) + \sqrt{(g + \alpha K/p)^2 - 1} \quad , \quad \lambda_2 = \frac{1}{\lambda_1} \tag{21}$$

The matrix eigenvectors of $\mathbf{T}_o$, $\mathbf{X}$, is given by Eq. (10) and the wave transfer matrix for an ordered span is

$$\mathbf{W}_o = \begin{bmatrix} \lambda_1 & 0 \\ 0 & \lambda_2 \end{bmatrix} \tag{22}$$

For a left- or a right-traveling wave, adjacent slopes are related by $\theta_{j+1} = e^{\pm\mu}\theta_j$, where μ is the propagation constant, defined as the logarithm of, say, the first eigenvalue of $\mathbf{T}_o$. Depending on frequency, μ is real or complex:

- For $g + \alpha K/p < -1$, $\lambda_{1,2}$ are real. Thus $\gamma = \ln|\lambda_1|$ and $\mu = \gamma + i\pi$, leading to wave attenuation with adjacent spans vibrating out of phase. If $g + \alpha K/p > 1$, then $\mu = \gamma$, leading to wave attenuation, with adjacent spans vibrating in phase. The corresponding frequencies define the *stopbands* of the multi-span beam.

- For $-1 < g + \alpha K/p < 1$, $\lambda_{1,2}$ are complex conjugate of modulus 1, with $\lambda_1 = \exp(i\xi)$. Thus $\gamma = \ln|\lambda_1| = 0$ and $\mu = i\xi$, $\xi \in [0, \pi]$. This leads to a non-attenuating propagating wave with a change in phase ξ at each span. The corresponding frequencies define the *passbands* of the structure. The natural frequencies of finite multi-span beams lie within the passbands.

- For $|g + \alpha K/p| = 1$, $\lambda_1 = \lambda_2 = \pm 1$, thus $\gamma = 0$ and $\mu = 0$ or $i\pi$. The corresponding frequencies define the *passband-stopband edges.*

The real and imaginary parts of the propagation constant are plotted in Fig. 3 versus frequency for two values of the torsional spring stiffness, K. Figure 4 displays the deflection shapes of typical traveling and attenuated waves (the wave shapes) at selected frequencies for an infinite beam.

In Fig. 3, note the regular pattern of alternating attenuation ($\gamma \neq 0$) and propagation ($\gamma = 0$) zones. The bounding frequencies of these bands can be related to the natural frequencies of a single span: the lower passband edges correspond to the natural frequencies of a span resting on supports of torsional stiffness $K/2$, while the upper passband edge frequencies coincide with the natural frequencies of a span *clamped* at both ends. In general, in the pth band a span vibrates primarily in its pth bending mode.

As expected, increasing the torsional stiffness of the supports reduces the width of the propagation bands through an increase in the lower passband edge frequencies. The upper edge frequencies do not depend on K because at these frequencies the wave shapes have zero slopes at the supports, as shown in Fig. 4. The narrowing of the passbands makes

sense because propagation becomes more difficult as the interspan coupling decreases, or as K increases. Weaker coupling also means a higher modal density for the multi-span beam and thus a higher sensitivity to periodicity-breaking imperfections (Pierre, 1988). Hence, we expect the interspan coupling, as determined by the torsional rigidity K, to be a key parameter in localization.

4. APPROXIMATE LOCALIZATION FACTORS IN THE DISORDERED CASE

Here we use statistical perturbative methods to approximate the localization factor of disordered multi-span beams in cases of strong and weak interspan coupling. We make the dimensionless length of the jth span, $\bar{l}_j$, a random variable of mean 1 and standard deviation σ, such that $\sigma \ll 1$, and define the dimensionless disorder as $\delta l_j = \bar{l}_j - 1$. When we need the probability density function, we assume a uniform distribution of width $w = \sqrt{3}\,\sigma$.

4.1 Weak Localization in the Strong Interspan Coupling Case

We take K to be small (possibly zero) and consider the small disorder as a perturbation, an approach we refer to as the classical perturbation method. We choose a wave formulation and expand the transmission coefficient in the disorder parameter to approximate the localization factor in Eq. (14). Except for the support stiffnesses that allow us to vary interspan coupling, the development is similar to that of Kissel (1988).

For frequencies inside the passbands, the wave transfer matrix for a span is, from Eqs. (7), (10), and (11):

$$(\mathbf{W}_j)_{11} = g_j + \frac{\alpha_j}{p}K + i\left(\frac{\alpha(1-g_j^2)}{2\alpha_j \sin\xi} + \frac{\alpha_j \sin\xi}{2\alpha} - \frac{\alpha g_j}{p\sin\xi}K - \frac{\alpha_j \alpha}{2p^2\sin\xi}K^2\right)$$

$$(\mathbf{W}_j)_{12} = i\left(\frac{\alpha(1-g_j^2)}{2\alpha_j \sin\xi} - \frac{\alpha_j \sin\xi}{2\alpha} - \frac{\alpha g_j}{p\sin\xi}K - \frac{\alpha_j \alpha}{2p^2\sin\xi}K^2\right) \tag{23}$$

where α_j and g_j are functions of the random length $\bar{l}_j$. We approximate the wave transfer matrix by expanding to the second-order in the small disorder δl_j

$$\mathbf{W}_j = \begin{bmatrix} e^{i\xi} & 0 \\ 0 & e^{-i\xi} \end{bmatrix} + \delta l_j \begin{bmatrix} a & b \\ b^* & a^* \end{bmatrix} + \frac{\delta l_j^2}{2}\begin{bmatrix} c & d \\ d^* & c^* \end{bmatrix} + O(\delta l_j^3) \tag{24}$$

To calculate the localization factor, we first multiply the $\mathbf{W}_j$'s to obtain the (1,1) element of the wave transfer matrix for N spans. This yields, to the second-order,

$$(\mathcal{W}_N)_{11} = e^{i\xi N}\left[1 + e^{-i\xi}\left(a\sum_{j=1}^{N}\delta l_j + c\sum_{j=1}^{N}\frac{\delta l_j^2}{2}\right)\right] \tag{25}$$

where we have dropped all terms involving products of at least two distinct random variables. The expectation of such terms is zero because the random lengths are independent variables.

Next, we take the modulus of the (1,1) term of the wave transfer matrix

$$|(\mathcal{W}_N)_{11}|^2 = 1 + 2\cos\xi\left(a_r\sum_{j=1}^{N}\delta l_j + c_r\sum_{j=1}^{N}\frac{\delta l_j^2}{2}\right)$$

$$+ 2\sin\xi \left(a_i \sum_{j=1}^{N} \delta l_j + c_i \sum_{j=1}^{N} \frac{\delta l_j^2}{2} \right) + a_r^2 \sum_{i=1}^{N} \delta l_j^2 + a_i^2 \sum_{j=1}^{N} \delta l_j^2 \tag{26}$$

where $a = a_r + ia_i$ and $c = c_r + ic_i$ are given in Appendix A. The next step is to take the logarithm of the modulus in Eq. (26) and expand it to the second order using $\ln(1+\epsilon) \simeq \epsilon - \frac{\epsilon^2}{2}$ with $|\epsilon| \ll 1$. At this stage we can either take the limit of the logarithm as $N \to +\infty$ or take its average for finite N (both procedures give the same result because of ergodicity). We choose the latter method and invoke the independence of the δl_j's. This yields, introducing the transmission coefficient from Eq. (13):

$$< \ln \left| \frac{1}{t_N} \right|^2 >= \left[-(c_r \cos\xi + c_i \sin\xi) - (a_r^2 + a_i^2) + 2(a_r \cos\xi + a_i \sin\xi)^2 \right] N\sigma^2 \tag{27}$$

Thus, from Eq. (14),

$$\gamma \simeq \gamma^{(c)} = \frac{\sigma^2}{2} \left[(c_r \cos\xi + c_i \sin\xi) + (a_r^2 + a_i^2) - 2(a_r \cos\xi + a_i \sin\xi)^2 \right] \tag{28}$$

where $\gamma^{(c)}$ is the "classical" approximation of the localization factor in the passbands for strong interspan coupling and weak disorder. Since the localization factor is proportional to the variance of the small disorder, the spatial attenuation is small, and we refer to this phenomenon as *weak localization.* We expect our approximation of γ to deteriorate as disorder increases, because we have retained only first-order terms in the variance. Better approximations could be obtained by considering more terms in the expansion.

Another observation is that the approximate localization factor becomes infinite for $\sin\xi = 0$, hence our perturbation approach breaks down at the passband-stopband edges. The approximation also deteriorates for K large, that is, for weak interspan coupling.

4.2 Strong Localization in Beams with Weak Interspan Coupling

We consider the case K large, that is, weak coupling between spans. The approximate localization factor, Eq. (28), breaks down because it is based upon a perturbation expansion in the small mistuning that ignores the other small parameter, the coupling. We can remedy this problem by *expanding in the small coupling.* However, to avoid degeneracy, we must include disorder in the unperturbed system, which then consists of decoupled spans of slightly different lenghts. This approach which we refer to as the modified perturbation method, makes physical sense because strongly localized vibrations are essentially perturbations of oscillations of decoupled spans (Pierre and Dowell, 1987).

We choose the vibration formulation of Section 2.3 to approximate the localization factor. In Eq. (20) the determinant can be calculated as the product of the eigenvalues of $\mathbf{A}$. In general these cannot be obtained analytically but for large K can be approximated using perturbation theory for the eigenvalue problem. We take $1/K$ as the perturbation parameter and write

$$\mathbf{A} = \mathbf{A}_o + \delta\mathbf{A} \tag{29}$$

where the unperturbed and perturbation matrices are

$$\mathbf{A}_o = \begin{bmatrix} \ddots & & & 0 \\ & 2K + \frac{pg_{j-1}}{\alpha_{j-1}} + \frac{pg_j}{\alpha_j} & & \\ 0 & & & \ddots \end{bmatrix}, \qquad \delta\mathbf{A} = \begin{bmatrix} \ddots & \ddots & & & 0 \\ \ddots & \ddots & \ddots & & \\ & -\frac{p}{\alpha_{j-1}} & 0 & -\frac{p}{\alpha_j} & \\ & & \ddots & \ddots & \ddots \\ 0 & & & \ddots & \ddots \end{bmatrix} \tag{30}$$

The eigenvalues of $\mathbf{A}_o$ are its diagonal elements and, assuming all span lengths are distinct, the eigenvectors are vectors $(\mathbf{e}_j)_{j=1,\cdots,N+1}$, where the jth element of $\mathbf{e}_j$ equals 1 and all other elements equal 0. The first-order perturbation of an eigenvalue of $\mathbf{A}$ is

$$\delta\lambda_j = \mathbf{e}_j^T \, \delta\mathbf{A} \, \mathbf{e}_j = 0 \tag{31}$$

Thus, to the first-order in $1/K$,

$$\det \mathbf{A} \simeq \left(K + \frac{pg_1}{\alpha_1}\right) \left\{ \prod_{j=2}^{N} \left(2K + \frac{pg_{j-1}}{\alpha_{j-1}} + \frac{pg_j}{\alpha_j}\right) \right\} \left(K + \frac{pg_N}{\alpha_N}\right) \tag{32}$$

From Eq. (20), the rate of decay for N spans is approximated as

$$\gamma_N \simeq \frac{1}{N}\sum_{j=1}^{N} \ln|\alpha_j| + \frac{1}{N}\sum_{j=2}^{N} \ln\left|\frac{2}{p} + \frac{1}{K}\left(\frac{g_j}{\alpha_j} + \frac{g_{j-1}}{\alpha_{j-1}}\right)\right|$$

$$+ \frac{N+1}{N}\ln K + \frac{1}{N}\ln p + \frac{1}{N}\ln\left|\frac{1}{p} + \frac{1}{K}\frac{g_1}{\alpha_1}\right| + \frac{1}{N}\ln\left|\frac{1}{p} + \frac{1}{K}\frac{g_N}{\alpha_N}\right| \tag{33}$$

The localization factor is the limit of γ_N as $N \to +\infty$. In Eq. (33) the terms that do not involve summations tend to zero, except one term that goes to $\ln K$. The first term in Eq. (33) tends to average of the random variable $\ln \alpha(\bar{l})$, where $\bar{l}$ is the random dimensionless span length, if we assume ergodicity. Next we consider the second term in Eq. (33). If we again assume that the lengths $\bar{l}_j$ form an ergodic sequence of independent and identically distributed random variables, we note that the argument in the logarithm essentially consists of two identical random variables, g_j/α_j and g_{j-1}/α_{j-1}. Thus we expect that in the limit $N \to \infty$ the second term in Eq. (33) tends to the average of the logarithm of twice the random variable $g(\bar{l})/\alpha(\bar{l})$ (with appropriate additive and multiplicative constants). This line of reasoning gives

$$\gamma \simeq \gamma^{(m)} = \ln K + \int_{-\infty}^{+\infty} \ln\left|\frac{2}{p}\alpha(\bar{l}) + \frac{2}{K}g(\bar{l})\right| \mathrm{pdf}(\bar{l})\, d\bar{l} \tag{34}$$

where "pdf" is the probability density function of the random length. For a uniform distribution of mean 1 and width $2w$, the above becomes

$$\gamma^{(m)} = \ln K + \frac{1}{2w}\int_{1-w}^{1+w} \ln\left|\frac{2}{p}\alpha(\bar{l}) + \frac{2}{K}g(\bar{l})\right| d\bar{l} \tag{35}$$

This closed-form approximation of the localization factor in the small coupling case can be easily evaluated numerically.

A few words are in order concerning the transition from Eq. (33) to Eq. (34). We have obtained an alternative result that accounts for the *two* random variables in the second logarithm term in Eq. (33), without using ergodicity, by taking the *average* of γ_N for *finite* beams. Clearly the result depends upon N but for N large can be approximated as

$$\gamma^{(m)} \simeq \ln K + \int_{-\infty}^{+\infty} \int_{-\infty}^{+\infty} \ln \left| \frac{2}{p}\alpha(\bar{l}) + \frac{1}{K}\left(g(\bar{l}) + g(\bar{l}')\frac{\alpha(\bar{l})}{\alpha(\bar{l}')}\right)\right| \mathrm{pdf}(\bar{l})\mathrm{pdf}(\bar{l}')d\bar{l}\, d\bar{l}' \qquad (36)$$

We have compared the localization factors given by Eq. (34) and Eq. (36) over wide parameter ranges. In all cases the single- and double-integral results were very close. The double integral, however, was much more expensive to calculate. In fact, its cost approached that of a brute force Monte Carlo simulation!

Moreover, at high frequencies (*e.g.*, in the tenth and higher bands), we noticed that the double-integral expression slightly underestimates the localization factor (the discrepancies were always less than 1%). We showed this by calculating γ_N in Eq. (33) and comparing it with the single and double integral results: for N large the results of Eq. (33) converge to the localization factor in Eq. (34). This leads us to believe that the correct expression of the localization factor is Eq. (34), although we cannot give a rigorous proof (we simply make an intuitive use of ergodicity). We conjecture that the double integral result is not strictly equivalent to it because it is an average for a finite chain and thus may include boundary terms.

5. ON MONTE CARLO SIMULATIONS AND WEAK AND STRONG LOCALIZATION

The approximations of the localization factor need to be validated by means of Monte Carlo simulations. We first discuss how these are carried out and then present a parametric study of confinement effects.

5.1 Monte Carlo simulations

These can be performed by the wave approach, Eq. (14), or the vibration formulation, Eq. (20). In both cases values of γ_N are calculated for N large and then ensemble-averaged over many realizations of disordered N-span beams. The random span lengths are obtained from a random number generator with a uniform distribution.

With the wave formulation the transmission coefficient t_N is computed by multiplying N random wave transfer matrices for each disordered beam. Then the logarithm of t_N is averaged over M realizations of multi-span beams. In our simulations we took $N = 100$ and $M = 1000$. This gave us a small error for the Monte Carlo estimates of γ and at the same time kept the computational time reasonable.

As pointed out by Kissel (1988), we noticed that very small values of the localization factor can be accurately simulated by averaging the logarithm of the transmission coefficient for a *single* disordered span. This approximation, however, quickly deteriorates as γ becomes larger. For $\gamma > 0.01$ at least several (say 20) transfer matrices should be multiplied before averaging. A tentative physical explanation is that the large reflections that occur at the supports in the strong localization case affect the dynamics of several neighboring spans, a mechanism that cannot be captured by using a single span in the simulations.

Two drawbacks of the wave simulation are (1) it is not accurate near the passband edges because the matrix $\mathbf{X}$ that defines the similarity transformation to the wave transfer

matrix is singular at the edges (this is because $\mathbf{T}_o$ has a double eigenvalue) and (2), its accuracy deteriorates as the localization factor becomes large, *i.e.* it does not handle strong localization well. Although we have observed the latter consistently in our simulations, we do not have a satisfactory explanation.

In cases where waves simulations are not adequate, we used the vibration formulation, Eq. (20). Clearly this approach does not work well for weak localization, because the decay per span is small and many spans are required to keep the influence of the boundary conditions to an acceptable level. Moreover, taking a very large number of spans N is not practical because the method requires solving eigenvalue problems of size N, which is computationally intensive. Hence vibration simulations are best suited to the strong localization case, such that the rate of decay is large and allows us to consider few spans. In these simulations we took beams with as many as 60 spans and averaged over 1000 beams.

5.2 Weak localization results

Here we examine localization for strong interspan coupling. Figures 5 and 6 display γ in terms of frequency for two values of K and for small disorder. Both classical perturbation (Eq. (28)) and wave simulation results are shown. We make the following observations.

While for the ordered beam there is no attenuation in the passbands, the disordered beam features spatial amplitude decay at all frequencies. The localization factor is minimum at the middle of the passbands of the ordered structure and increases rapidly as the stopbands are approached. In fact, we noted in Section 4.1 that the classical approximation of γ goes to infinity at the passband edges. This means that incident waves and normal modes whose frequency is near the band edges will localize much more than those whose frequency is near midband. Thus, as observed by Kissel (1988), the degree of localization depends strongly on frequency within a passband in the strong coupling case. We also observe that localization effects increase with frequency from passband to passband and that localization increases for all frequencies as K increases, or as the interspan coupling decreases. The latter is illustrated in Table 1: for $K = 100$ there is substantial confinement even for a ten-span beam.

Figure 5 shows the excellent agreement between the classical perturbation method and the Monte Carlo simulations for $K = 0$. Note from Fig. 6 that the classical perturbation analysis start to break down for $K = 100$, indicating the transition from weak to strong localization. In general we observed that the classical perturbation results overpredict the simulation results in four cases: as K increases, near the band edges, as the passband number increases and, although not shown here, as the disorder increases. These observations make sense because the classical perturbation method treats the small disorder as a perturbation and thus can only be accurate for small γ. The approach fails whenever the localization factor becomes large, in which cases the modified perturbation scheme must be used.

The results in Fig. 5 tell us that the effects of disorder are small for strong interspan coupling. To illustrate these effects, consider the case where all span lengths are within 1% percent of the mean and the supports have no torsional rigidity. At the middle of the first passband[1], Table 1 gives the localization factor as $\gamma_{mid} = 28 \times 10^{-5}$. On the average the vibration amplitude decays as $\exp(-\gamma N)$, where N is the span number. This means that if the first span vibrates with a unit amplitude the 100th span's expected amplitude is 0.972. Obviously the confinement effect of disorder is very weak here. Moreover, the localization factor is for an *infinite* and *undamped* structure, and such effects of disorder would most

[1] We define the midband frequencies when the wave number equals $\pi/2$.

likely be obscured by the dissipation and the boundary conditions present in all engineering structures. In fact, this is precisely why we were unable to verify the small values of γ by vibration simulations: several thousands of spans were required to offset boundary effects and only wave simulations, which do not include boundary conditions, could be used.

Fig. 7 illustrates some wave shapes for a disordered infinite beam in a case of moderate localization. Notice that for the same excitation frequency, the wave shapes of the ordered beam are propagating while those of the disordered beam are localized.

5.3 Strong localization results

Here we present results for weak interspan coupling. Figure 8 shows the localization factor in the vicinity of the first frequency band for $K = 1000$. First, we note the excellent agreement over the frequency range shown between the modified perturbation and the simulations results. Next, we observe that for K large γ is large and thus confinement is severe. Finally, for very strong localization (*e.g.*, $\sigma = 1.5\%$), Fig. 8 shows that γ varies little with frequency throughout the passband, contrary to the weak localization case.

Figure 9 displays the variation of the localization factor at the first midband frequency in terms of the torsional stiffness K, for a small disorder $\sigma = 0.577\%$. Observe that in the first region (approximately $K \in [0, 100]$) the classical perturbation results follow the Monte Carlo simulations closely. In this weak localization regime the variation of γ with K is parabolic-like. The second region, $K \in [100, 300]$, corresponds to the transition from weak to strong localization, where neither perturbation scheme gives good results. As K increases, the modified perturbation results approach the Monte Carlo simulations, indicating the occurrence of strong localization for weak interspan coupling. Equation (35) tells us that in this third region γ varies nearly logarithmically with K. The variation of γ shown in Fig. 9 would be similar if plotted versus the disorder σ instead of K.

It has been shown by Pierre and Dowell (1987) for simple periodic systems that localization depends primarily on the disorder to coupling ratio. It is of interest to investigate whether this finding holds for multi-span beams, *i.e.* whether γ depends on $\sigma/(1/K)$ (and, of course, on frequency). Since this cannot be readily deduced from the perturbation results, Eqs. (28) and (35), we performed a numerical parametric study. Figure 10 displays iso-localization factor lines in the (K, σ)-plane, obtained by Monte Carlo simulations. Simple calculations for several points show that the product σK is nearly constant along each iso-γ line, and thus these have a nearly hyperbolic shape. This suggests that γ is primarily a function of the disorder to coupling ratio.

6. EFFECT OF FREQUENCY ON LOCALIZATION

In Section 5 we have examined the variation of the localization factor with frequency *inside* a passband. Here we study confinement effects as the frequency increases from passband to passband. To that end we consider the localization factor at the midband frequencies.

For strong coupling, $K = 0$, we can obtain a closed-form approximation of the localization factor at midband. Approximating the midband frequency of the ith band by $\overline{\omega}_{mid} \simeq [(i + 1/4)\pi]^2$, Eq. (28) can be shown to give

$$\gamma^{(c)}_{mid} \simeq \frac{1}{2}(i + \frac{1}{4})^2 \pi^2 \sigma^2 \tag{37}$$

The derivation is outlined in Appendix B. The validity of Eq. (37) is illustrated in Fig. 11, which displays the localization factor at the first 15 midband frequencies. Note the good

agreement between the Monte Carlo simulations and both the classical approximation of γ (Eq. (28)) and its further approximation (Eq. (37)). As expected, the classical perturbation scheme overpredicts γ as i increases.

Equation (37) shows that the degree of localization *grows linearly with frequency* from passband to passband or, equivalently, increases with the square of the passband number. This means that a transition from weak to strong localization takes place as the passband number increases. This result makes sense because at higher frequencies the spans are dynamically stiffer and thus become less coupled than at low frequencies, which in turn results in stronger confinement. Note, however, that γ increases much less rapidly for the multi-span beam than for an assembly of spring-coupled beams (Cha and Pierre, 1990), where γ varies as i^8 and the transition to strong confinement is very rapid.

Figure 12 displays the localization factor at midband frequencies in terms of the passband number for various values of K and σ. We clearly observe the transition from weak to strong localization as i increases for the case $K = 50$ and $\sigma = 1.5\%$: the simulation results nicely depart from the classical approximation of γ to approach the modified approximation as frequency increases. For small K and small σ there is weak confinement over the first 15 bands, although strong localization would eventually occur as i increases further. For large K strong localization occurs already in the first band, and consequently in all bands. However, note that for strong localization γ remains practically constant as i increases. This contrasts with the case of an assembly of coupled beams, where γ increases with the logarithm of i in the strong localization regime (Cha and Pierre, 1990).

We also explored localization at very high frequencies, even though the Euler-Bernoulli model we use is questionable (in this case the Timoshenko model of Lust *et al.* (1990) may be better suited). Figure 13 displays localization factors at midband versus passband number. For weak interspan coupling we observe that while there is a very small increase of γ in the first 50 passbands, a substantial drop takes place as i keeps increasing. This means that some de-localization takes place at very high frequencies. This unexpected variation of the localization factor is predicted remarkably closely by the modified perturbation method. We also observe de-localization for strong interspan coupling in Fig. 13, taking place after the transition from weak to strong localization.

We tentatively explain this de-localization by noting that at very high frequencies the wavelengths of the deflection patterns are comparable in magnitude to typical variations in support spacing. This means that such waves may propagate more easily through the supports. Indeed, we observe in Fig. 13 that de-localization takes place for $i \sim 100$, corresponding to a dimensionless half-wavelength of 0.01. In terms of orders of magnitudes this compares well with the disorder in the support spacing ($w = 1\%$). This conjecture is confirmed by Fig. 14, which displays the localization factor at high passband numbers for various K and σ. We notice that for $w = 1\%$ de-localization takes place near values of i that are multiples of 100 and for $w = 1.5\%$ near values of i multiples of 66. Figure 14 also shows that this pattern is the same for both strong and weak inter-span coupling.

7. CONCLUSIONS

In this paper we have explored the effects of slight randomness in support spacing on the dynamics of multi-span beams on rigid supports. We have shown that the key parameter that governs the sensitivity to disorder is the dynamic interspan coupling. For weak coupling disorder alters drastically the beam's dynamics: waves and vibrations that transmit freely through the ordered structure become trapped near the excitation source.

We have characterized the degree of localization by the average rate of spatial decay of the vibration amplitude and obtained analytical approximations of this localization factor for weak and strong interspan coupling. We have found that for strong coupling localization effects are weak and minimum at the midband frequencies. For weak coupling the localization factor is large and increase with the logarithm of the support stiffness. Moreover, even for strong static coupling, localization effects increase nearly linearly with frequency from passband to passband, and a transition from weak to strong localization occurs if the passband number is high enough. Thus, severe confinement is unavoidable for strong static coupling if the frequency is large enough. In the strong localization regime the increase of the localization factor with frequency is quite moderate, and some de-localization is observed at very high frequencies.

ACKNOWLEDGEMENT

This work is supported by National Science Foundation Grant No. MSS-8913196, Dynamic Systems and Control Program. Dr. Elbert L. Marsh is the grant monitor.

REFERENCES

Anderson, P. W., 1958, "Absence of Diffusion in Certain Random Lattices," *Physical Review*, Vol. 109, pp. 1492-1505.

Bendiksen, O. O., 1987, "Mode Localization Phenomena in Large Space Structures," *AIAA Journal*, Vol. 25, No. 9, pp. 1241-1248.

Bouzit, D., 1988, "Vibration Confinement Phenomena in Disordered Multi-span Beams: A Probabilistic Investigation," *Master's Thesis, The University of Michigan.*

Brillouin, L., 1953, *Wave Propagation in Periodic Structures*, Second Edition, Dover Publication, New York.

Cai, G. Q., and Lin, Y. K., 1990, "Localization of Wave Propagation in Disordered Periodic Structures," AIAA Paper 90-1216, *Proceedings of the AIAA Dynamics Conference*, Long Beach, California.

Cha, P. D., and Pierre, C., 1990, "Vibration Localization by Disorder in Assemblies of Mono-Coupled, Multi-Mode Component Systems," AIAA Paper 90-1213, *31th AIAA Dynamics Specialists Conference*, Long Beach, California.

Cornwell, P. J., and Bendiksen, O. O., 1989, "Localization of Vibrations in Large Space Reflectors," *AIAA Journal*, Vol. 27, No. 2, pp. 219-226.

Faulkner, M. G., and Hong, D. P., 1985, "Free Vibration of a Mono-Coupled Periodic System," *Journal of sound and Vibration*, Vol. 99, No. 1, pp. 29-42.

Heckl, M., 1964, "Investigation on the vibration of grillages and other simple beam structures," *Journal of the Acoustical Society of America*, Vol. 7, No. 36, pp. 1335.

Hodges, C. H., 1982, "Confinement of Vibration by Structural Irregularity," *Journal of Sound and Vibration*, Vol. 82, No. 3, pp. 411-424.

Hodges, C. H., and Woodhouse, J., 1983, "Vibrations Isolation from Irregularity in a Nearly Periodic Structure: Theory and Measurements," *Journal of the Acoustical Society of America* , Vol. 74, No. 3, pp. 894-905.

Kissel, G. J., 1988, "Localization in Disordered Periodic Structures," *Ph.D. Dissertation, Massachusetts Institute of Technology.*

Lin, Y. K., and McDaniel, T. J., 1969, "Dynamics of Beam-Type Periodic Structures," *ASME Journal of Engineering for Industry*, Vol. 91, Series B, No. 4, pp. 1133-1141.

Lin, Y. K., and Yang, J. N., 1974, "Free Vibrations of a Disordered Periodic Beam," *ASME Journal of Applied Mechanics*, Vol. 41, No. 2, pp. 383-391.

Lust, S. D., Friedmann, P. P. and Bendiksen, O. O., 1990, "Mode Localization in Multi-span Beams," AIAA Paper 90-1214, *Proceedings of the AIAA Dynamics Conference*, Long Beach, California.

Mead, D. J., 1970, "Free Wave Propagation in Periodically Supported Infinite Beams," *Journal of Sound and Vibration*, Vol. 11, No. 2, pp. 181-197.

Mead, D. J., 1971, "Vibration Response and Wave Propagation in Periodic Structures," ASME, *Journal of Engineering for Industry*, Vol. 93. Series B, No. 3, pp. 783-792.

Mead, D. J., 1975, "Wave Propagation and Natural Modes in Periodic Systems: I. Mono-Coupled Systems," *Journal of Sound and Vibration*, Vol. 40, No. 1, pp. 1-18.

Mead, D. J., and Markuš, Š., 1983, "Coupled Flexural-Longitudinal Wave Motion in a Periodic Beam," *Journal of Sound and Vibration*, Vol. 90, No. 1, pp. 1-24.

Miles, J. W., 1956, "Vibration of Beams on Many Supports," *Journal of Engineering Mechanics Division, ASCAE*, Vol. 82, No. EM1, pp. 1-9.

Pierre, C., 1988, "Mode Localization and Eigenvalue Loci Veering Phenomena in Disordered Structures" *Journal of Sound and Vibration*, Vol. 126, No. 3, pp. 485-502.

Pierre, C., 1990, "Weak and Strong Vibration Localization in Disordered Structures: A Statistical Investigation," *Journal of Sound and Vibration*, Vol. 139, No. 1, pp. 111–132.

Pierre, C., and Dowell, E. H., 1987, "Localization of Vibrations by Structural Irregularity," *Journal of Sound and Vibration*, Vol. 114, No. 3, pp. 549-564.

Pierre, C., Tang, D. M., and Dowell, E. H., 1987, "Localized Vibrations of Disordered Multi-Span Beams: Theory and Experiment," *AIAA Journal*, Vol. 25, No. 9, pp. 1249-1257.

Sen Gupta, G., 1970, "Natural Flexural Waves and the Normal Modes of Periodically-Supported Beams and Plates," *Journal of Sound and Vibration*, Vol. 13, No. 1, pp. 89-101.

Tassilly, E., 1987, "Propagation of Bending Waves in a Periodic Beam," *International Journal of Engineering Science*, Vol. 25, No. 1, pp. 85-94.

APPENDIX A

$$g = \frac{\sinh p \cos p - \cosh p \sin p}{\sinh p - \sin p}$$

$$f = \sqrt{1 - g^2}$$

$$s_1 = (\sinh p + \sin p)/2$$

$$s_3 = (\sinh p - \sin p)/2$$

$$s_4 = \sinh p \sin p$$

$$c_2 = (\cosh p - \cos p)/2$$

$$c_4 = (\cosh p \cos p - 1)/2$$

$$\alpha = \frac{c_4}{s_3}$$

In the mistuned case, the functions for the jth span are obtained by replacing p by its randomized equivalent $p_j = p\bar{l}_j$. In the following (') denotes a derivative with respect to the random length evaluated at the mean $\bar{l}_o = 1$. The subscripts r and i refer to real and imaginary parts, respectively.

$$g' = -p\frac{s_4 + gc_2}{s_3}$$

$$g'' = -p^2 g \frac{2c_4 + s_1 s_3}{s_3^2}$$

$$f' = \frac{f}{2\alpha} p(g - \frac{c_4 c_2}{s_3^2}) + \frac{p\alpha}{4f} \frac{\sinh^2(p)\cos(p) - \cosh(p)\sin^2(p)}{s_3^2}$$

$$f'' = -\frac{fp^2}{2\alpha}[\frac{s_4 + 2gc_2}{s_3} - c_4 \frac{2c_2^2 - s_1 s_3}{s_3^3}] + \frac{\alpha p^2}{2f} \frac{2s_3 g^2 - s_1 s_4}{s_3^2} - f\left(\frac{f'}{f} - \frac{\alpha'}{\alpha}\right)$$

$$\cos\xi = g + \frac{\alpha}{p}K$$

$$\sin\xi = \sqrt{1 - (g + \alpha K/p)^2}$$

$$a_r = g' + \frac{\alpha'}{p}K$$

$$a_i = \frac{ff'}{\sin\xi} + \frac{f^2\alpha'}{2\alpha\sin\xi} + \frac{\alpha'\sin\xi}{2\alpha} - \frac{g'\alpha}{p\sin\xi}K - \frac{\alpha\alpha'}{2p^2\sin\xi}K^2$$

$$c_r = g'' + \frac{\alpha''}{p}K$$

$$c_i = \frac{ff''}{\sin\xi} + \frac{f^2}{\sin\xi}\left(\frac{f'}{f} - \frac{\alpha'}{\alpha}\right) + \frac{f^2\alpha''}{2\alpha\sin\xi} + \frac{\alpha''\sin\xi}{2\alpha} - \frac{g''\alpha}{p\sin\xi}K - \frac{\alpha\alpha''}{2p^2\sin\xi}K^2$$

APPENDIX B: LOCALIZATION FACTOR AT MIDBAND

For a multi-span beam, we approximate the frequency parameter at mid-band, $\sqrt{\bar{\omega}_{mid}}$, by the average of that of a pinned-pinned span and that of a clamped-clamped span. This yields, in the ith band, for i sufficiently large (*i.e.* $i \geq 2$):

$$\bar{\omega}_{mid} \simeq (i + \frac{1}{4})^2 \pi^2$$

The circular and hyperbolic functions at the mid-band frequency can be calculated by replacing $p = \sqrt{\bar{\omega}_{mid}}$ by $(i + \frac{1}{4})\pi$,

$$\begin{aligned} \cos(\sqrt{\bar{\omega}_{mid}}) \simeq \sin(\sqrt{\bar{\omega}_{mid}}) &\simeq \frac{1}{\sqrt{2}} \cos(i\pi) \\ \cosh(\sqrt{\bar{\omega}_{mid}}) \simeq \sinh(\sqrt{\bar{\omega}_{mid}}) &\simeq (\sinh(\frac{\pi}{4}) + \cosh(\frac{\pi}{4})) \cosh(i\pi) \end{aligned}$$

The functions and their derivatives defined in Appendix A can be simplified by noting that for sufficiently large i the hyperbolic functions are very large compared to the other terms. We obtain the simplified expressions:

$$\begin{array}{lll} g = 0, & g' = -\sqrt{2}(i + \frac{1}{4})\pi \cos(i\pi), & g'' = 0 \\ f = 1, & f' = 0, & f'' = -(i + \frac{1}{4})^2 \pi^2 \end{array}$$

Substituting the above into Eq. (28) and letting $K = 0$, we obtain the simple expression:

$$\gamma_{mid} \simeq \frac{1}{2}\sigma^2(g'^2 + f'') = \frac{1}{2}\sigma^2(i + \frac{1}{4})^2 \pi^2$$

K	$\bar{\omega}_{mid}$	γ_{mid}	A_1	A_{10}	A_{100}
0.0	16.1214	0.00028	1.0	0.9971	0.9721
25.0	21.0006	0.01354	1.0	0.8737	0.2592
100.0	21.9575	0.17201	1.0	0.1790	3.10^{-8}

Table 1. Average amplitude attenuation at the first midband in disordered N-span beams, for $\sigma = 0.577\%$ (by Monte Carlo simulations).

List of Figures

Fig. 1 Multi-span beam on knife-edge supports with torsional springs.
Fig. 2 One span.
Fig. 3 Propagation constant versus frequency for an ordered multi-span beam, for $K = 0$ (——) and $K = 30$ (—).
Fig. 4 Traveling and attenuated wave shapes at selected frequencies for an ordered infinite beam, for $K = 0$.
Fig. 5 Localization factor versus frequency in the first three passbands for $K = 0$ and $\sigma = 0.577\%$, by classical perturbation method (—) and Monte Carlo simulations (o). The decay constant of the ordered beam is shown (——).
Fig. 6 Localization factor versus frequency in the first three passbands for $K = 100$ and $\sigma = 0.577\%$, by classical perturbation method (—) and Monte Carlo simulations (o). The decay constant of the ordered beam is shown (——).
Fig. 7 Localized and traveling wave shapes for an infinite disordered (—) and ordered (——) multi-span beams, respectively, for $K = 50$. In the disordered case $\sigma = 1.0\%$.
Fig. 8 Localization factor versus frequency in the first passband for $K = 1000$, by modified perturbation method (—) and Monte Carlo simulations (o). The decay constant of the ordered beam is shown (——).
Fig. 9 Localization factor at the first midband frequency versus torsional spring constant, for $\sigma = 0.577\%$, by modified perturbation method (—), classical perturbation method (——), and Monte Carlo simulations (o).
Fig. 10 Localization factor at the first midband frequency in the (K, σ)-plane, by Monte Carlo simulations.
Fig. 11 Localization factor at the midband frequencies versus passband number for $K = 0$ and $\sigma = 0.577\%$, by Monte Carlo simulations (o), classical perturbation method ($\cdot$), and approximate classical perturbation result ($\square$).
Fig. 12 Localization factor at the midband frequencies versus passband number, for various values of K and σ, by Monte Carlo simulations (o), classical perturbation method ($*$), and modified perturbation method ($+$).
Fig. 13 Localization factor at the midband frequencies versus passband number for $\sigma = 0.577\%$ and various K, by Monte Carlo simulations (o), classical perturbation method ($+$), and modified perturbation method ($\cdot$).
Fig. 14 Localization factor at the midband frequencies versus passband number by modified perturbation method, for $\sigma = 0.577\%$ or $w = 1.0\%$ ($\cdot$), and for $\sigma = 0.866\%$ or $w = 1.5\%$ ($\triangle$).

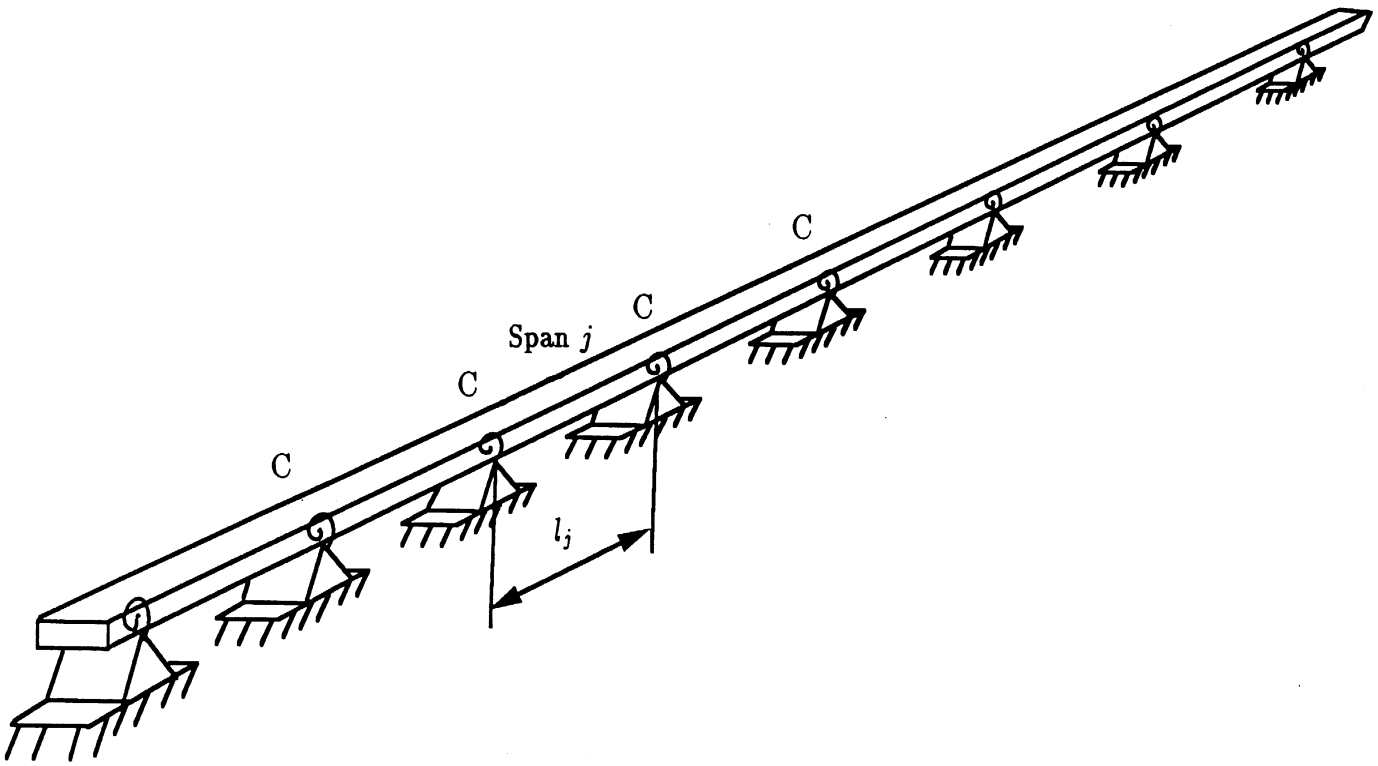

Figure 1. Multi-span beam on knife-edge supports with torsional springs.

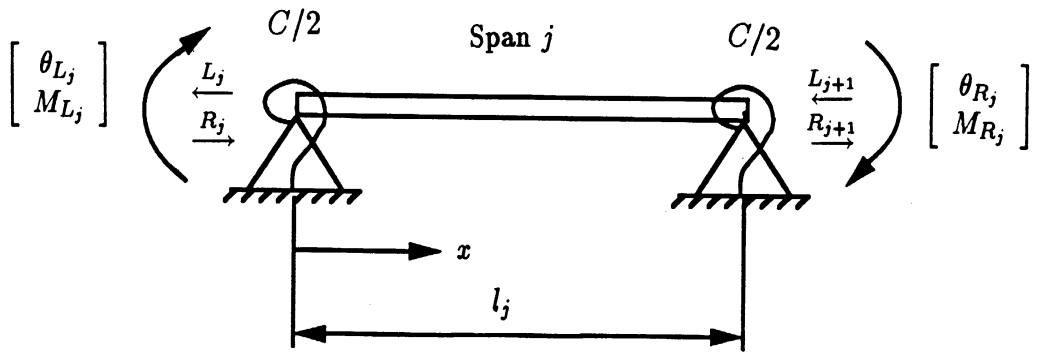

Figure 2. One span.

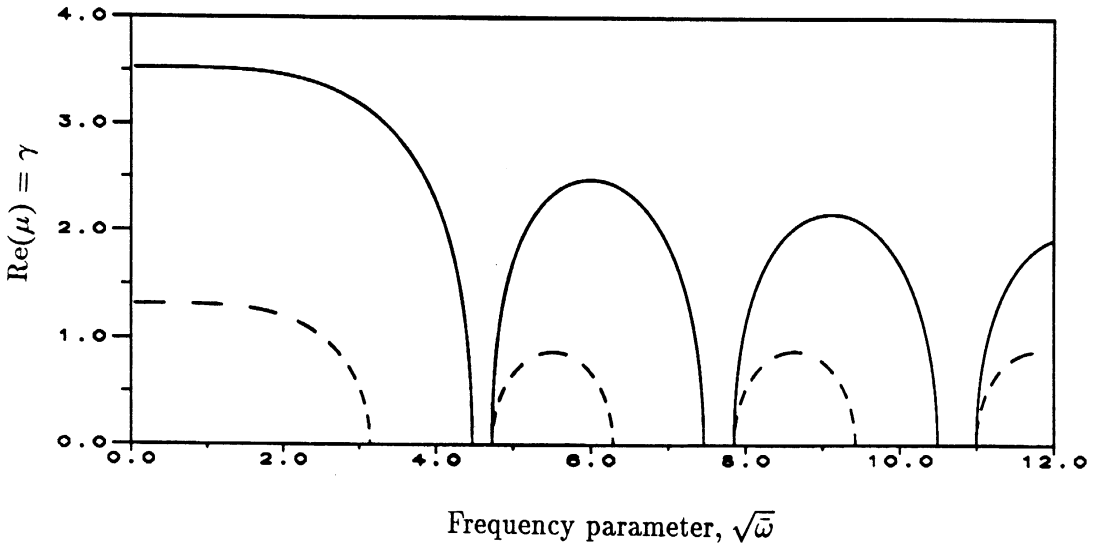

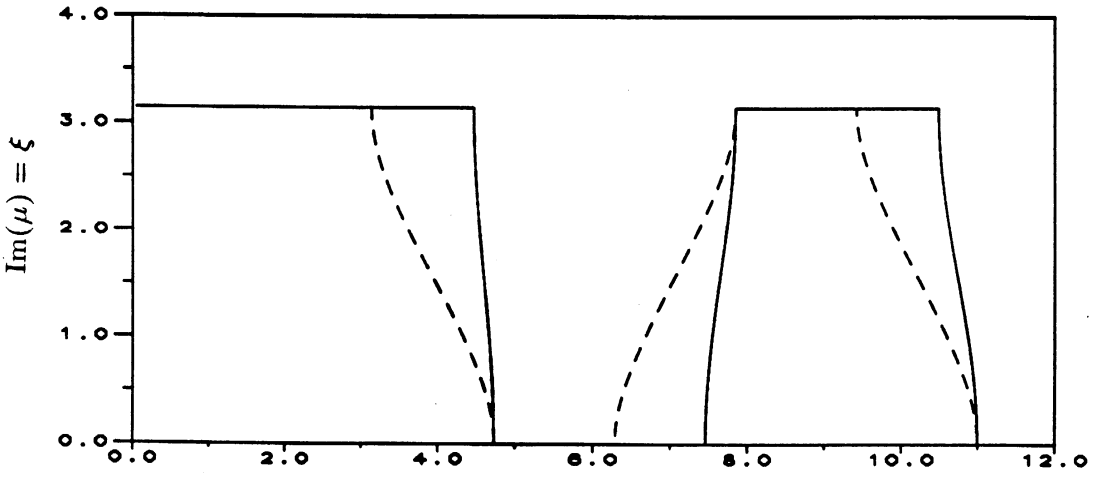

Figure 3. Propagation constant versus frequency for an ordered multi-span beam, for $K = 0$ (– –) and $K = 30$ (—).

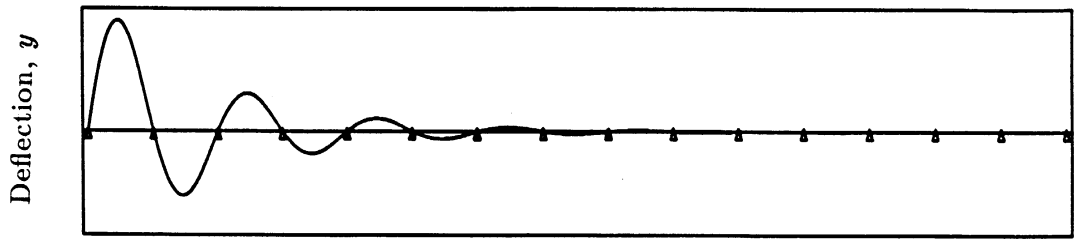

$\sqrt{\bar{\omega}} = 3.00$ (in the first stopband)

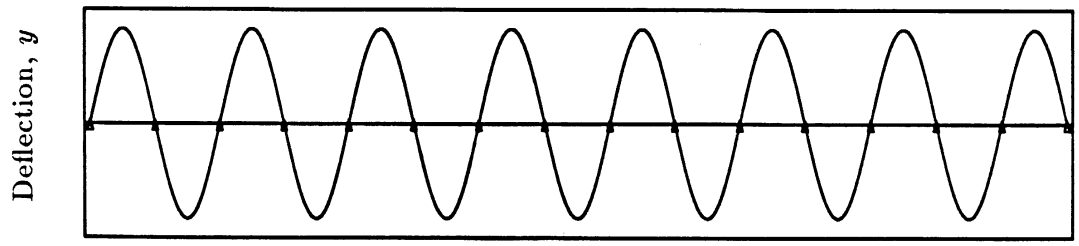

$\sqrt{\bar{\omega}} = 3.1416$ (at the lower edge of the first passband)

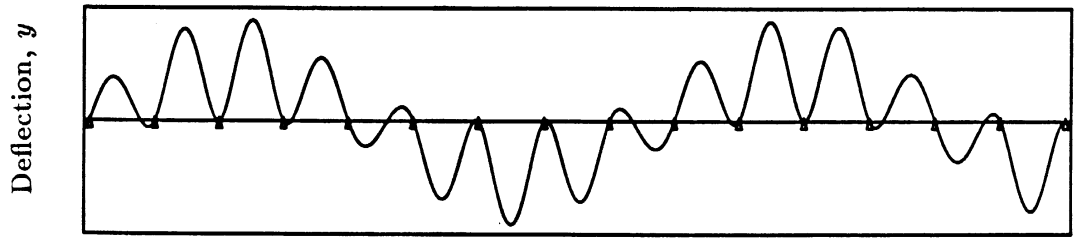

$\sqrt{\bar{\omega}} = 4.50$ (in the first passband)

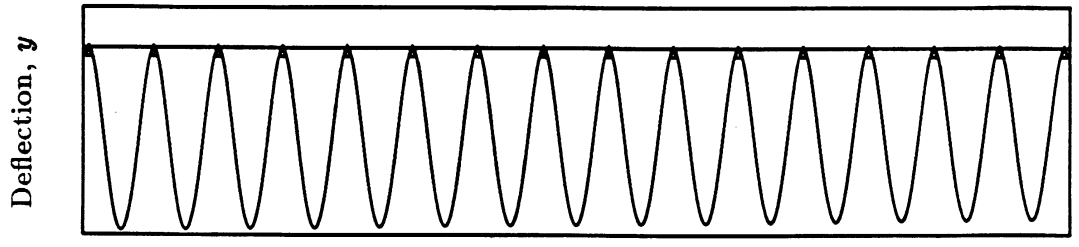

$\sqrt{\bar{\omega}} = 4.73005$ (at the upper edge of the first passband)

Figure 4. Traveling and attenuated wave shapes at selected frequencies for an ordered infinite beam, for $K = 0$.

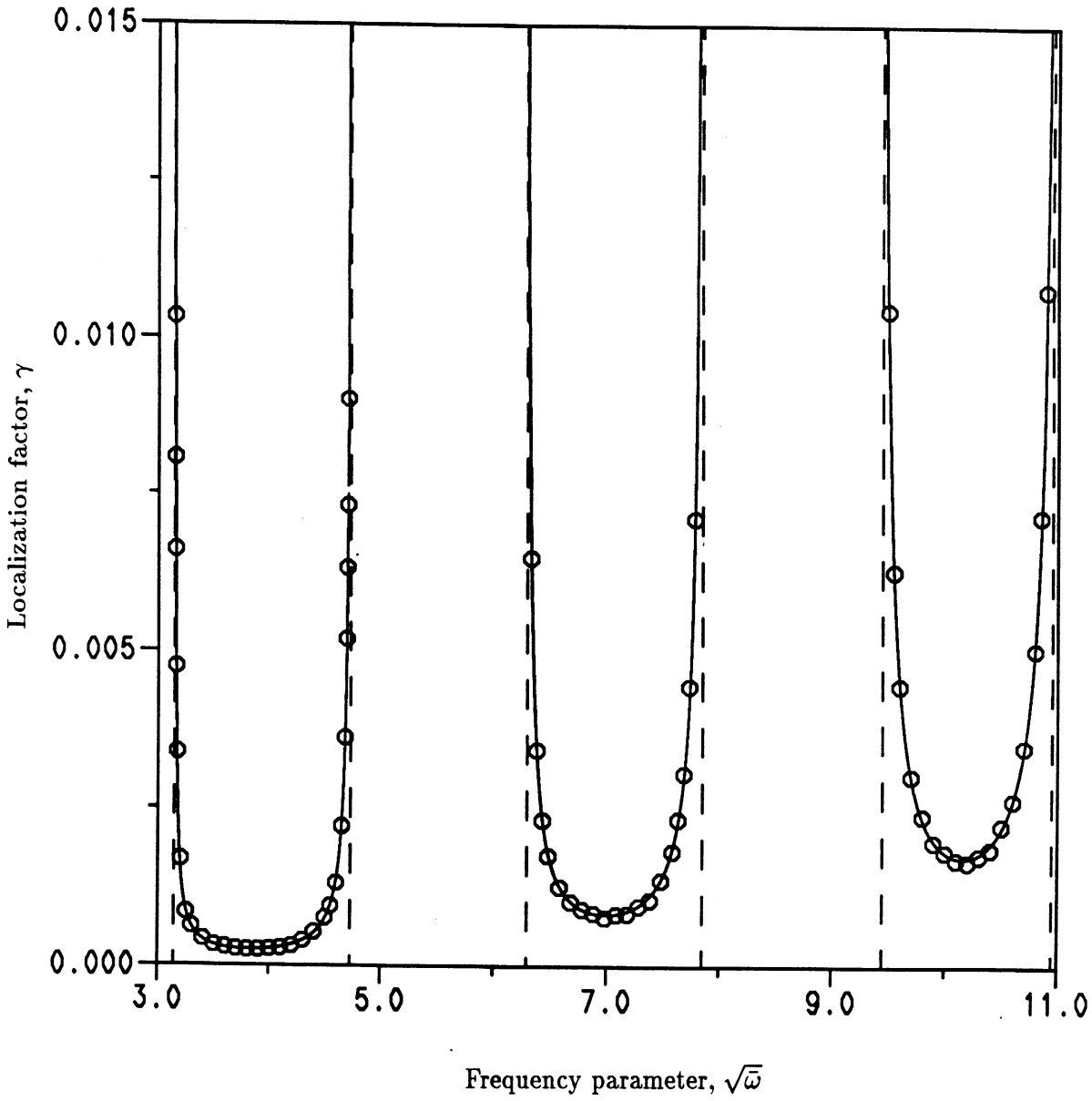

Figure 5. Localization factor versus frequency in the first three passbands for $K = 0$ and $\sigma = 0.577\%$, by classical perturbation method (—) and Monte Carlo simulations (o). The decay constant of the ordered beam is shown (– –).

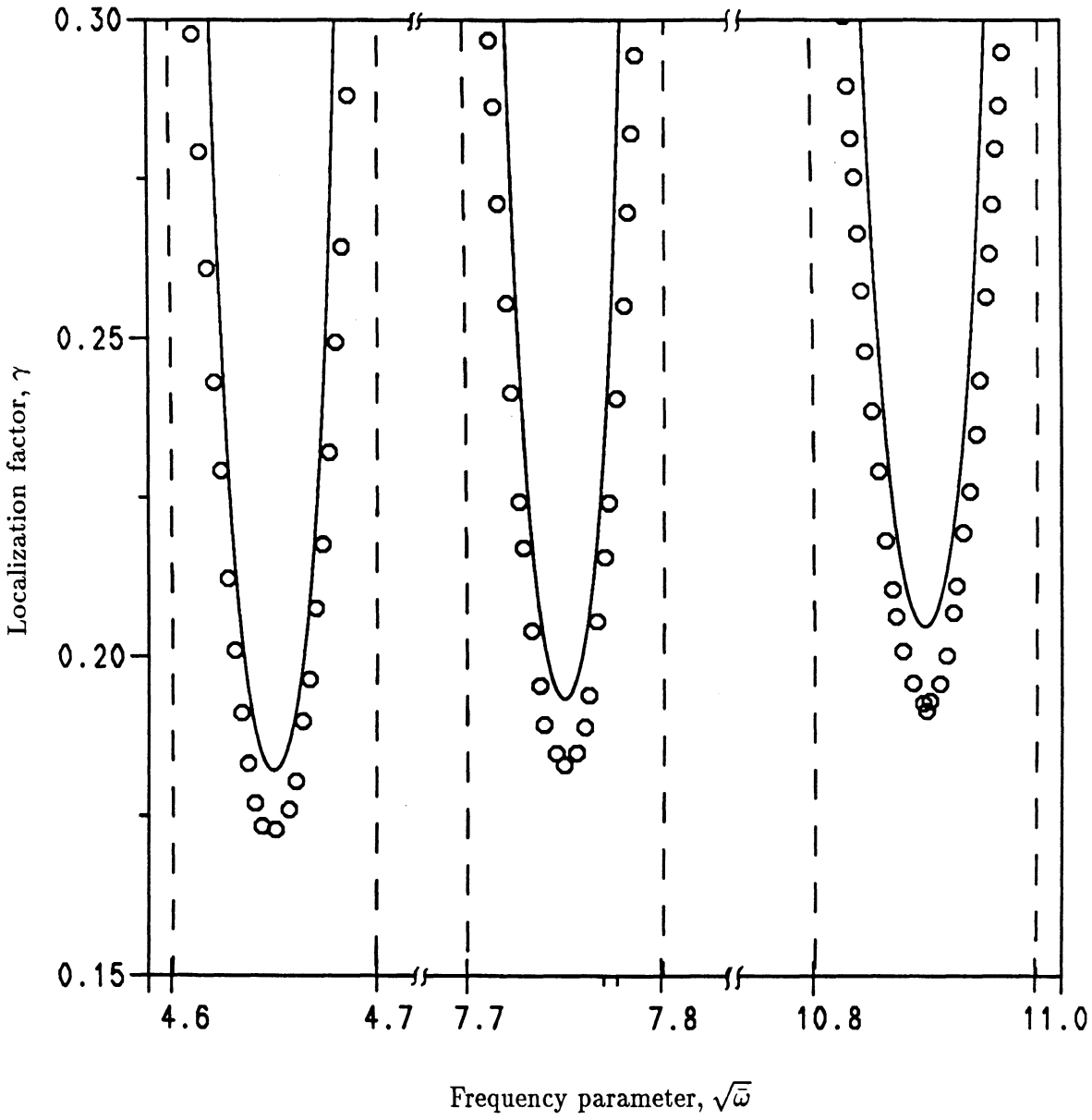

Figure 6. Localization factor versus frequency in the first three passbands for $K = 100$ and $\sigma = 0.577\%$, by classical perturbation method (—) and Monte Carlo simulations (o). The decay constant of the ordered beam is shown (– –).

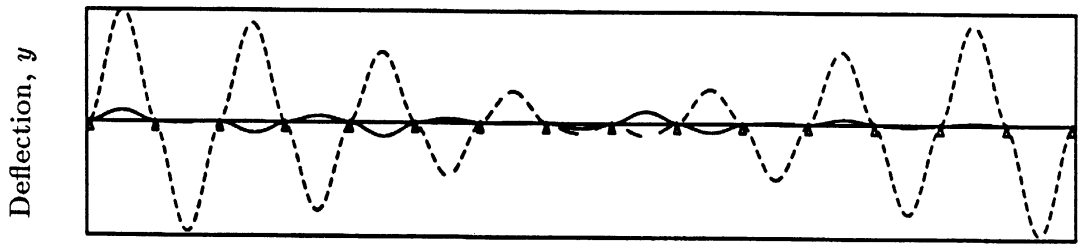

$\sqrt{\bar{\omega}} = 4.5647$ (near the lower edge of the first passband)

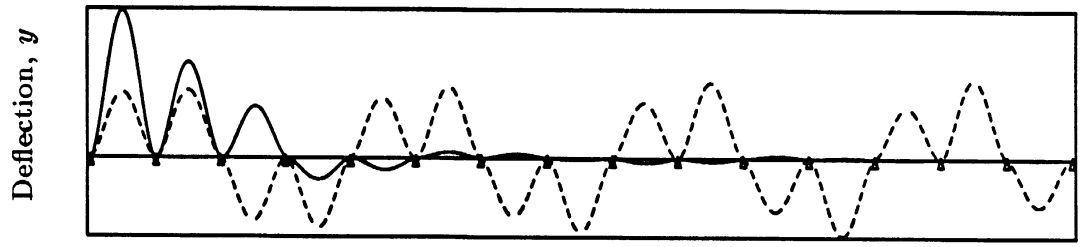

$\sqrt{\bar{\omega}} = 4.6465$ (near the first midband)

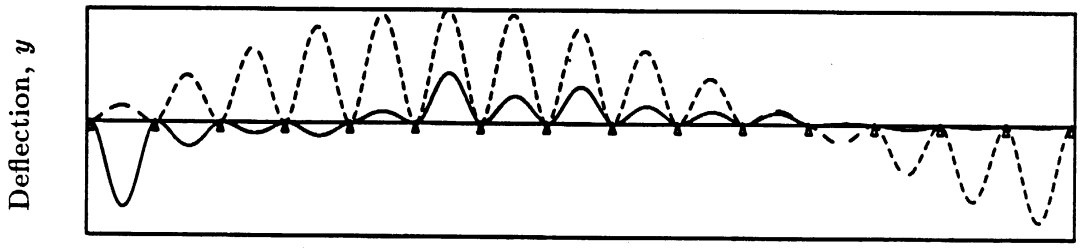

$\sqrt{\bar{\omega}} = 4.7265$ (near the upper edge of the first passband)

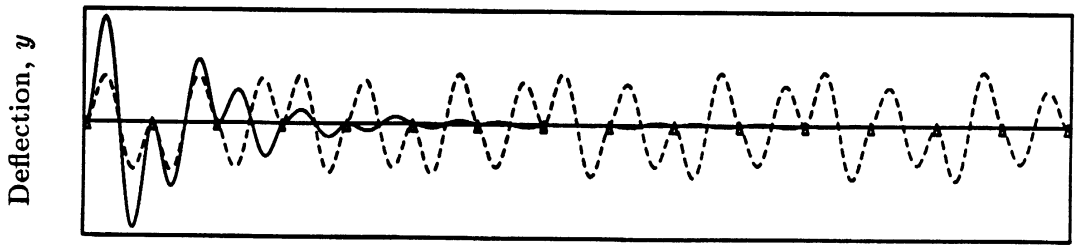

$\sqrt{\bar{\omega}} = 7.7220$ (near the second midband)

Figure 7. Localized and traveling wave shapes for an infinite disordered (—) and ordered (– –) multi-span beams, respectively, for $K = 50$. In the disordered case $\sigma = 1.0\%$.

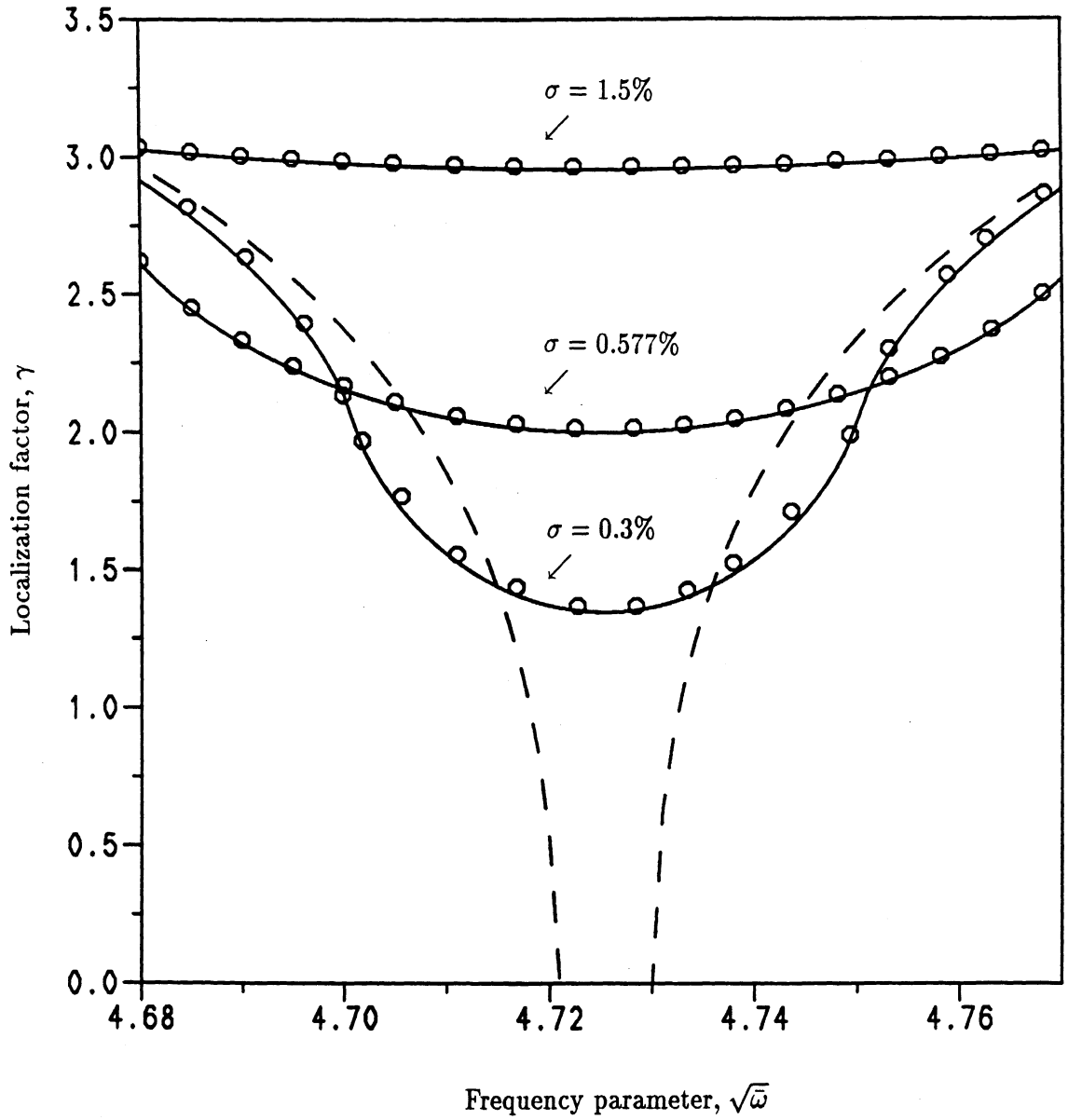

Figure 8. Localization factor versus frequency in the first passband for $K = 1000$, by modified perturbation method (—) and Monte Carlo simulations (o). The decay constant of the ordered beam is shown (– –).

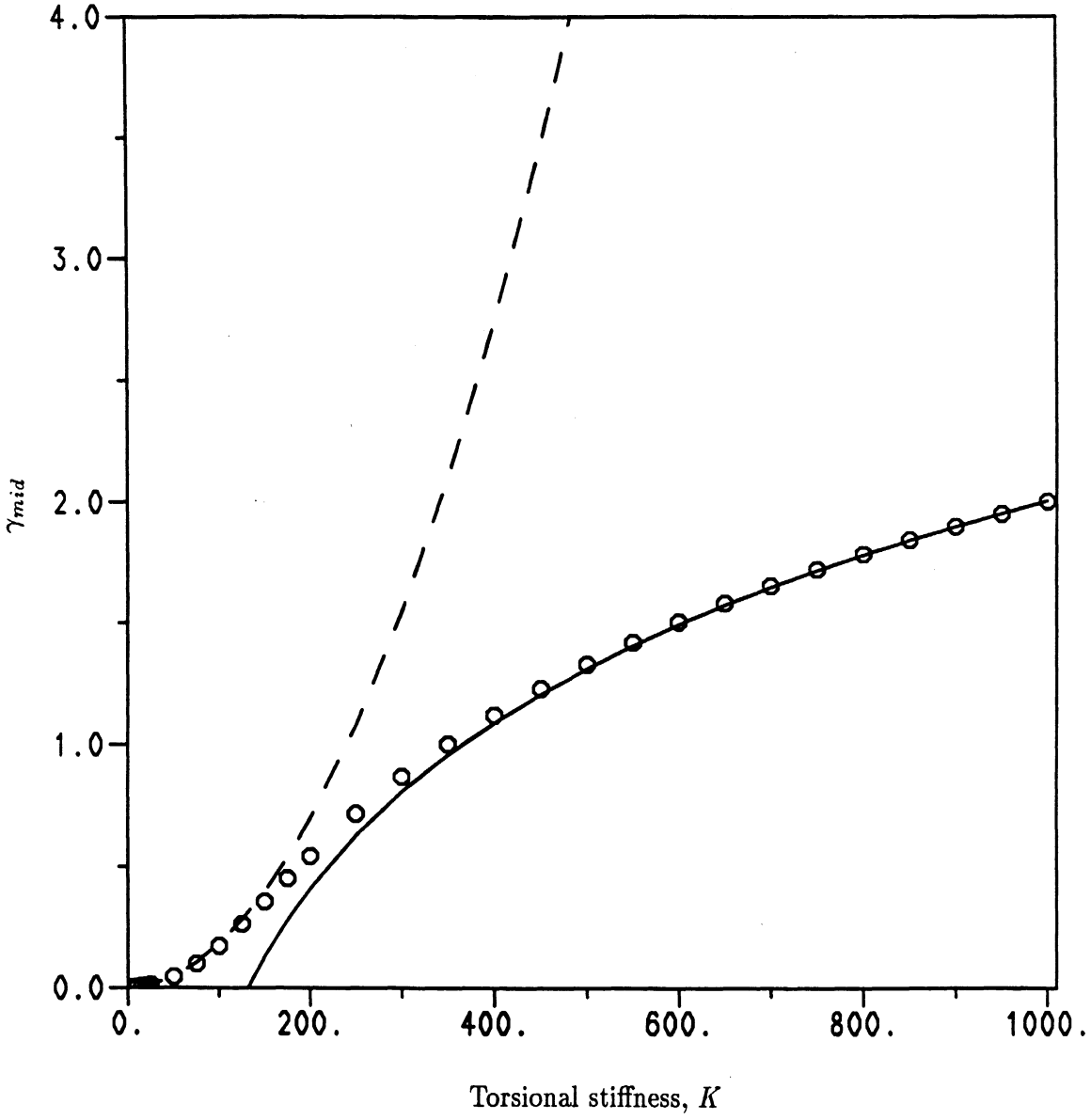

Figure 9. Localization factor at the first midband frequency versus torsional spring constant, for $\sigma = 0.577\%$, by modified perturbation method (—), classical perturbation method (– –), and Monte Carlo simulations (o).

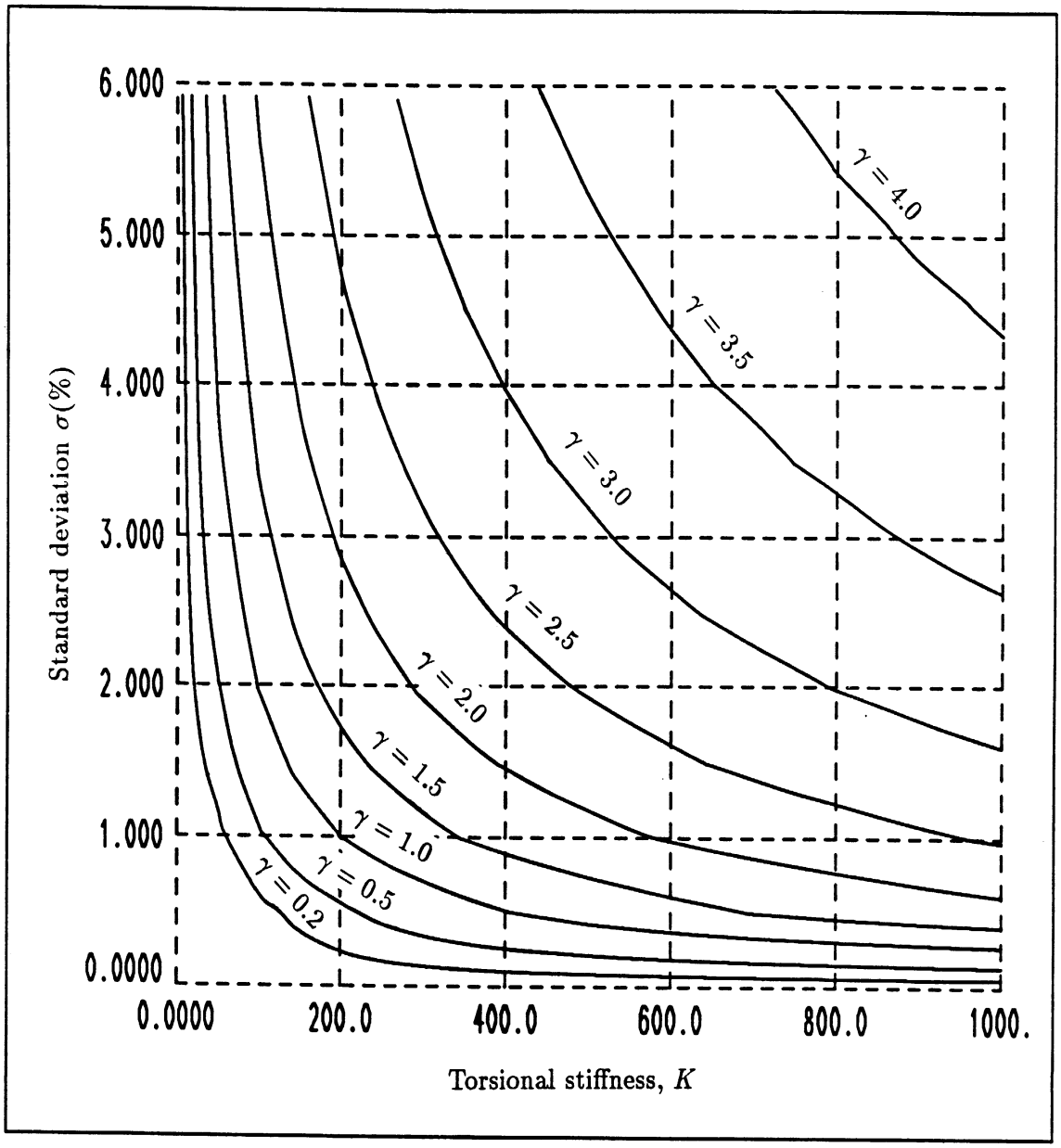

Figure 10. Localization factor at the first midband frequency in the (K, σ)-plane, by Monte Carlo simulations.

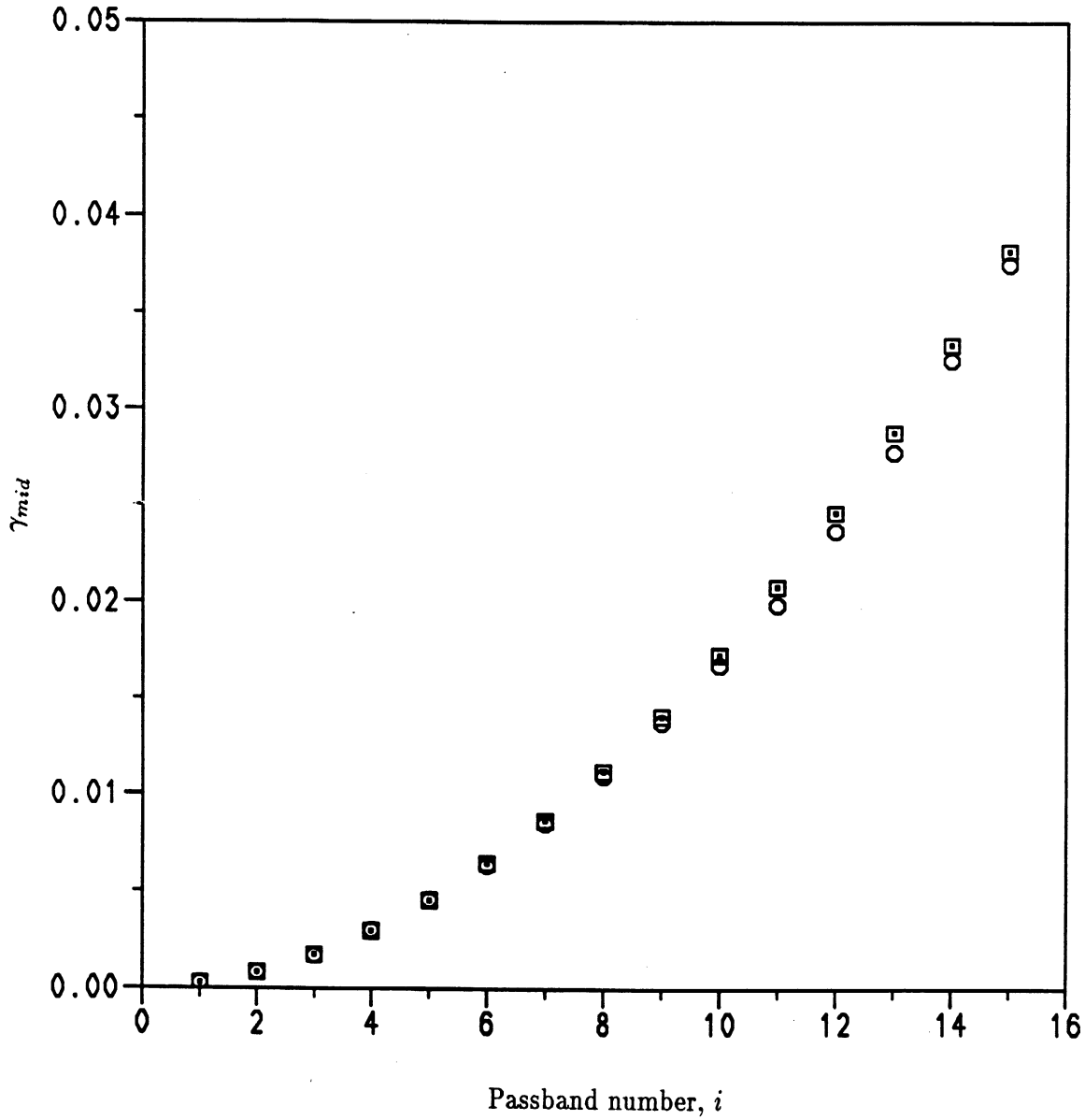

Figure 11. Localization factor at the midband frequencies versus passband number for $K = 0$ and $\sigma = 0.577\%$, by Monte Carlo simulations (o), classical perturbation method (·), and approximate classical perturbation result (□).

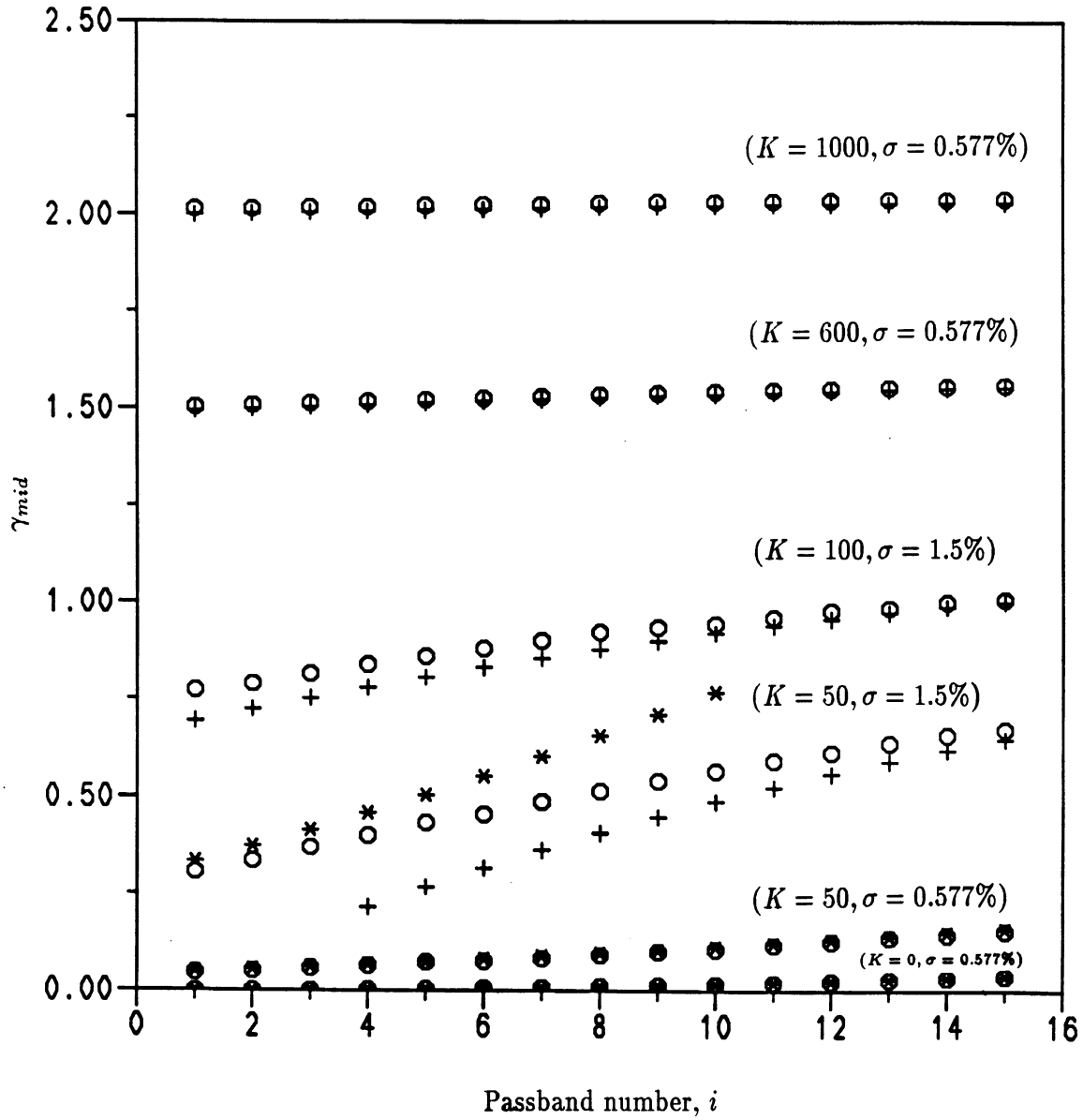

Figure 12. Localization factor at the midband frequencies versus passband number, for various values of K and σ, by Monte Carlo simulations (o), classical perturbation method (*), and modified perturbation method (+).

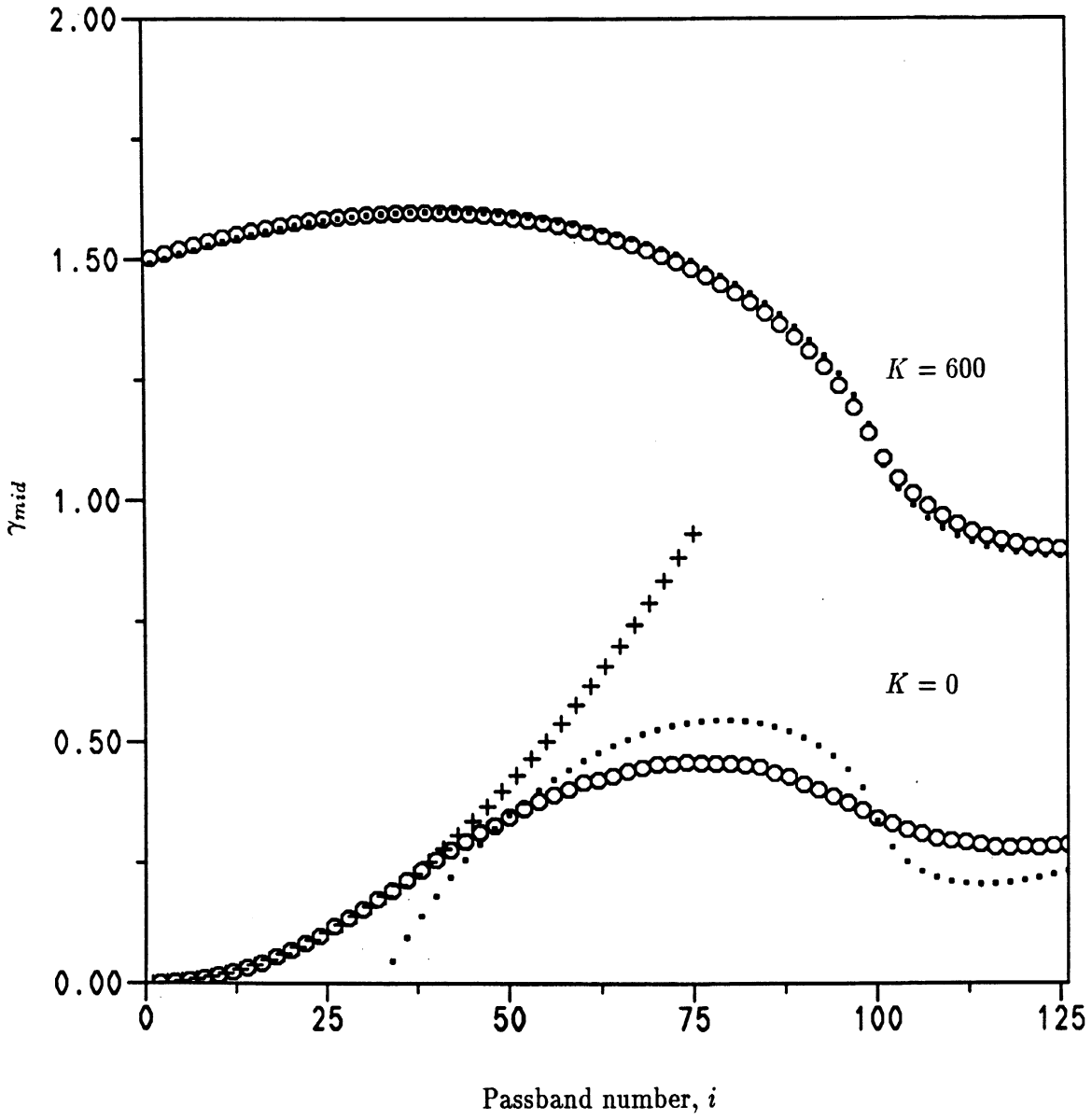

Figure 13. Localization factor at the midband frequencies versus passband number for $\sigma = 0.577\%$ and various K, by Monte Carlo simulations (o), classical perturbation method (+), and modified perturbation method ($\cdot$).

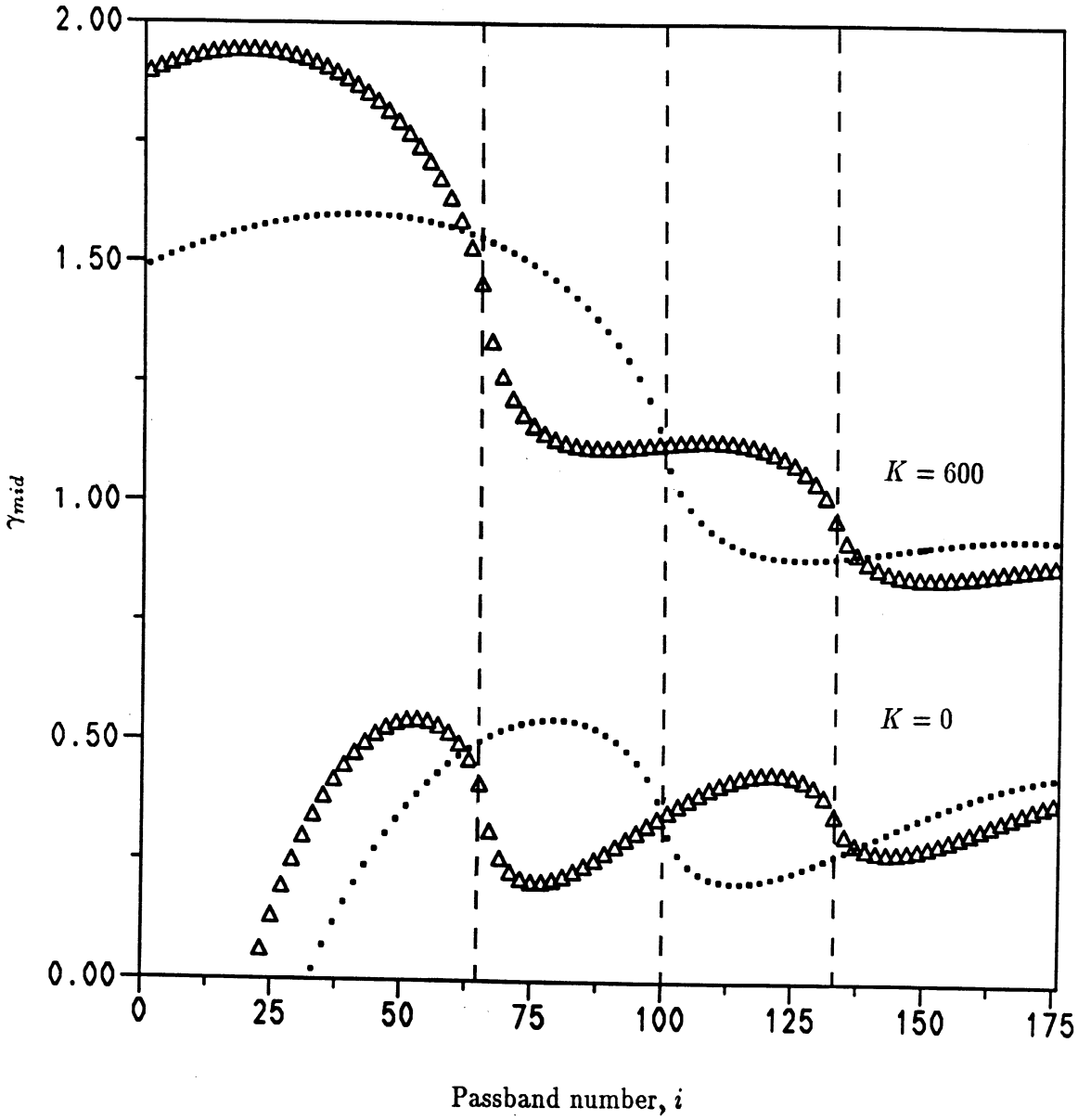

Figure 14. Localization factor at the midband frequencies versus passband number by modified perturbation method, for $\sigma = 0.577\%$ or $w = 1.0\%$ ($\cdot$), and for $\sigma = 0.866\%$ or $w = 1.5\%$ ($\triangle$).